encompasses a wide spectrum of conditions associated with over-accumulation of fat in the liver, ranging from simple steatosis (SS) to nonalcoholic steatohepatitis (NASH), and cirrhosis [2]. Although SS typically follows a benign non-progressive clinical course, NASH may eventually develop into cirrhosis and HCC. To date, a liver biopsy remains the gold standard for the diagnosis of NASH [3]. However, since the biopsy procedures carry the risk of mortality [4,5], the noninvasive identification of biomarkers, that can provide reliable differential diagnoses for the characterization of liver diseases, is desirable.

Metabolomics, which can be defined as measurement of the levels of all cellular metabolites, has emerged as a powerful new tool for discovering new low molecular weight biomarkers. Its utility has been demonstrated by the identification of new biomarkers for prostate cancer [6], Parkinson's disease [7], type 2 diabetes mellitus [8], acute myocardial ischemia [9], and pre-eclampsia [10].

Recently, we developed new metabolomic profiling approaches based on capillary electrophoresis mass spectrometry [11] and capillary electrophoresis–time-of-flight mass spectrometry (CE–TOFMS) [12–14]. The efficacy of CE–TOFMS was demonstrated by the discovery of ophthalmate (γ-glutamyl-2-aminobutyrylglycine) as a biomarker; in mice, reduced glutathione (GSH) depletion produced acetaminophen-induced hepatotoxicity [12,14]. In this study, to discover new noninvasive biomarkers for human liver diseases, we comprehensively analyzed the serum metabolites in a total of 248 samples from patients with nine types of liver disease or gastric cancer (GC) and from normal individuals using our metabolomic approaches, and found increased levels of γ-glutamyl dipeptides in the majority of the liver diseases. Moreover, we found that γ-glutamyl dipeptides were synthesized via the ligation of glutamate with various amino acids and amines by the γ-glutamylcysteine synthetase (GCS), an enzyme that is feedback-inhibited by GSH, and that the levels of γ-glutamyl dipeptides were indicative of the amount of GSH production. The concentrations of serum γ-glutamyl dipeptides varied with the stage and type of liver disease and can, therefore, act as new biomarkers for liver diseases. Here, we report that a highly specific set of γ-glutamyl dipeptides, alone or in combination with transaminases and methionine sulfoxide, can effectively distinguish specific liver diseases from other hepatic injuries and healthy control samples.

Materials and methods

Serum samples

A total of 248 serum samples were obtained from three institutes, Yamagata University Hospital (YUH; Yamagata, Japan), University of Tokyo Hospital (UTH; Tokyo, Japan) and Shonai Hospital (SH; Tsuruoka, Japan). The 162 YUH cases comprised 53 healthy controls (C) and patients with drug-induced liver injury (DI; $n = 10$), asymptomatic hepatitis B virus infection (AHB; $n = 9$), chronic hepatitis B (CHB; $n = 7$), hepatitis C with persistently normal alanine transaminase (CNALT; $n = 10$), chronic hepatitis C (CHC; $n = 24$), cirrhosis type C (CIR; $n = 10$), HCC ($n = 19$), SS ($n = 9$) and NASH ($n = 11$). The 75 UTH cases comprised four controls and patients with DI ($n = 17$), AHB ($n = 7$), CHB ($n = 7$), CNALT ($n = 8$), CHC ($n = 11$), CIR ($n = 8$) and HCC ($n = 13$). The 11 SH cases were all GC patients. Written informed consent was obtained from all the participants and the study protocol conformed to the ethical guidelines of the 1975 Declaration of Helsinki as reflected in a priori approval by the appropriate institutional review boards of YUH, UTH, and SH. The study subjects were patients with viral liver diseases, drug-induced hepatotoxicity or NAFLD who were referred to the Department of Gastroenterology and Hepatology at YUH, UTH, or SH.

Clinical diagnosis

All the healthy controls had normal liver function and no viral hepatitis infection, and none were alcoholics. The AHB and CNALT patients were confirmed to have normal liver function and to be positive for hepatitis B surface (HBs) antigen and hepatitis B virus (HBV) DNA, or for anti-hepatitis C virus (HCV) antibodies and HCV RNA, respectively. DI was diagnosed based on abnormal values on biochemical tests, absence of other hepatic diseases, and a history of treatment with drugs suspected of being probable causes of DI. The suspected medications were different, and the biochemical test results in each patient normalized after their withdrawal.

CHC and CIR were diagnosed on the basis of physical examination, biochemical tests, ultrasonography, and CT findings. Some patients with chronic hepatitis provided informed consent for a liver biopsy, and the procedure was performed to confirm the accuracy of the diagnosis. The diagnosis of CHB and CHC was based on increased ALT levels (above the upper limit of the normal range) in at least two blood samples assayed over a 6-month period, and the presence of detectable HBs antigen and HBV DNA or detectable anti-HCV antibodies and HCV RNA, respectively. HCV infection was causative in all cirrhosis patients, and they manifested symptoms of portal hypertension, such as splenomegaly, esophageal varices, encephalopathy, or ascites.

The diagnosis of HCC was based on ultrasonography, CT, and MRI findings that revealed features typical of HCC. HCV was causative in all cases, and the α-fetoprotein (AFP) and protein induced by vitamin K antagonist (PIVKA)-II levels were assayed in all HCC patients.

All of the SS and NASH patients underwent liver biopsy. The tissue samples were stained with hematoxylin–eosin, reticulin, and Masson trichrome; and examined by the same experienced pathologist who was blinded to the clinical data. The histological criterion for the diagnosis of NAFLD was the presence of fatty changes in hepatocytes. When hepatocytes exhibited macrovesicular steatosis, the differential diagnosis was SS or NASH. The criteria for a diagnosis of steatohepatitis were the presence of lobular inflammation and either ballooning cells or perisinusoidal/pericellular fibrosis, in addition to steatosis in the liver specimen. No patient with autoimmune hepatitis, primary biliary cirrhosis, sclerosing cholangitis, hemochromatosis, α1-antitrypsin deficiency, Wilson's disease, or alcoholic liver injury was included. All patients with GC were diagnosed by pathologic studies of biopsy tissues.

Analytical and statistical technologies for biomarker discovery

Using a total of 237 samples from YUH (training cohort, $n = 162$) and UTH (validation cohort, $n = 75$) (Table 1), we performed CE–TOFMS for a comprehensive analysis of the metabolite changes to discover new biomarkers in the diagnosis of human liver diseases. To facilitate peak identification and quantification, we analyzed 162 metabolic standards listed in the KEGG LIGAND database [15] before analyzing the samples. Global mass scanning over a 50–1000 m/z range was applied in the CE–TOFMS mode [12]. To focus on γ-glutamyl peptides, we employed a highly sensitive method using liquid chromatography electrospray tandem mass spectrometry (LC–MS/MS) with multiple reactions monitoring for analyses of the patient serum samples. The Kruskal–Wallis test and Dunn's post-test were used to assess the statistical significance of differences among C, DI, AHB, CHB, CNALT, CHC, CIR, and HCC. The Mann–Whitney test was used to evaluate the statistical significance of differences between SS and NASH. The algorithm of the feature selection for the multiple logistic regression (MLR) models is described in the Supplementary data.

Results

Discovery of γ-glutamyl dipeptides in serum by metabolomic profiling

The CE–TOFMS analysis quantified the levels of 49 metabolites in the serum samples (Supplementary Tables 1 and 2) and revealed increases in many compounds in most liver diseases. We identified these compounds as γ-glutamyl dipeptides (e.g., γ-Glu-Gly, γ-Glu-Ala, γ-Glu-Ser, γ-Glu-Val, γ-Glu-Thr, γ-Glu-Taurine, γ-Glu-Leu, γ-Glu-Gln, γ-Glu-Lys, γ-Glu-Glu, γ-Glu-Met, γ-Glu-His, γ-Glu-Phe, γ-Glu-Arg, γ-Glu-Citrulline, γ-Glu-Tyr, and γ-Glu-Trp) by comparing their migration times and exact molecular

Table 1. Summary of patient information.

Clinical information		Training cohort (n = 162)	Defect no.	Validation cohort (n = 75)	Defect no.	*p* value
Age (years)						
	Median	61	0	66	0	0.47
	Interquartile range	51-73	0	55-70	0	
Sex (n)	Male	73	0	52	0	0.0007*
	Female	89	0	23	0	
AST (UL^{-1})						
	C	21.5 ± 5.40	0	25.3 ± 3.60	0	0.074
	DI	274 ± 567	0	81.2 ± 84.9	0	0.15
	AHB	25.0 ± 6.81	2	23.9 ± 6.90	0	0.71
	CHB	109 ± 164	0	150 ± 146	0	0.0059
	CNALT	24.1 ± 3.80	0	23.8 ± 6.00	0	0.72
	CHC	62.8 ± 65.3	0	110 ± 51.0	0	0.0010
	CIR	54.6 ± 27.1	0	58.0 ± 26.1	0	0.69
	HCC	71.3 ± 52.8	0	35.0 ± 24.5	0	0.0010
	SS	41.2 ± 11.5	0			
	NASH	78.6 ± 48.0	0			
ALT (UL^{-1})						
	C	17.7 ± 4.70	0	25.0 ± 8.30	0	0.062
	DI	253 ± 343	0	115 ± 132	0	0.15
	AHB	26.6 ± 18.6	2	23.1 ± 5.60	0	0.40
	CHB	117 ± 162	0	173 ± 131	0	0.0060
	CNALT	17.9 ± 4.10	0	21.5 ± 3.60	0	0.074
	CHC	79.4 ± 81.0	0	160 ± 116	0	0.0036
	CIR	40.7 ± 21.9	0	57.3 ± 42.4	0	0.69
	HCC	57.9 ± 58.8	0	25.0 ± 21.6	0	0.0026
	SS	72.2 ± 24.5	0			
	NASH	121 ± 140	0			
γ-GTP						
	C	20.7 ± 8.60	0	—	4	—
	DI	190 ± 236	0	46.2 ± 29.5	5	0.010
	AHB	31.1 ± 24.1	2	—	7	—
	CHB	52.8 ± 38.1	1	—	7	—
	CNALT	150 ± 5.70	0	—	8	—
	CHC	48.5 ± 36.4	0	—	11	—
	CIR	28.8 ± 17.9	0	49.6 ± 53.1	0	0.17
	HCC	51.2 ± 31.1	0	—	13	—
	SS	61.8 ± 43.7	0			
	NASH	98.7 ± 99.1	0			
AFP						
	CHC	6.40 ± 7.40	3	—	11	—
	CIR	35.1 ± 71.8	0	14 ± 15.6	0	0.63
	HCC	9.79×10^2 ± 1.73×10^3	0	7.04×10^3 ± 2.52×10^4	0	0.024
PIVKA-II						
	HCC	1.57×10^2 ± 1.87×10^2	0	7.78×10^3 ± 2.77×10^4	0	0.022

*Chi-square test. The others *p* values were obtained by the Mann–Whitney *U*-test.

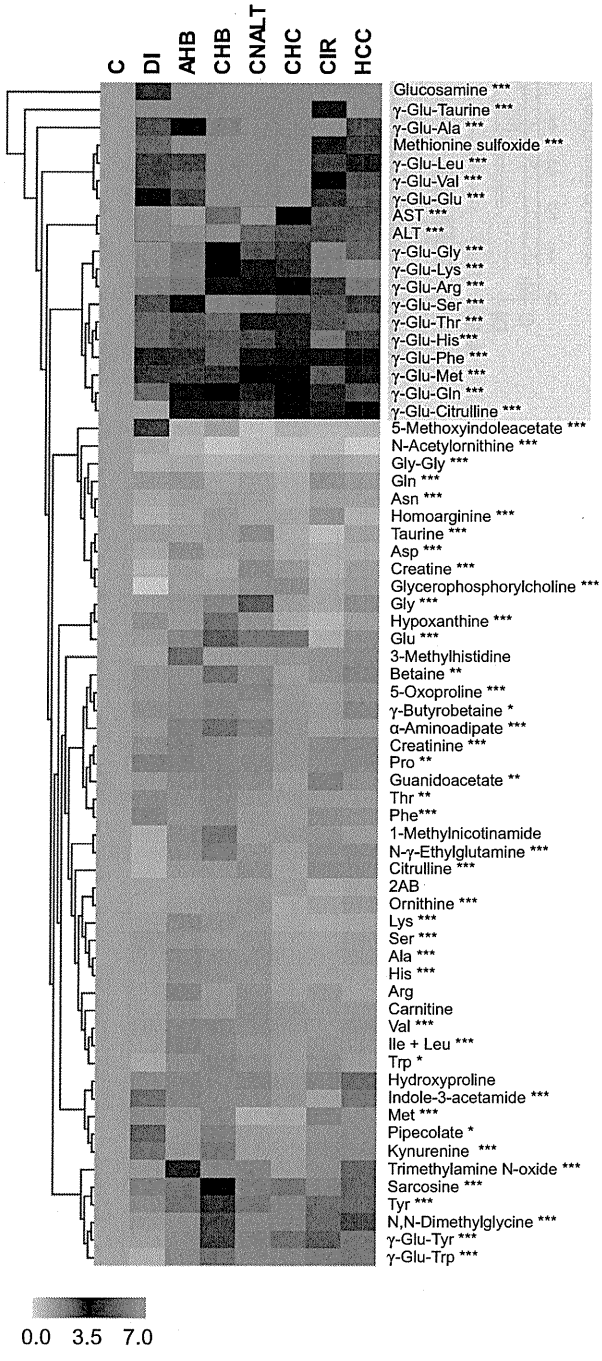

Fig. 1. Heat map representing the hierarchical clustering of 67 compounds in serum samples from controls and patients with various types of liver disease in both cohorts. Each row shows data for a specific metabolite or transaminase, and each column shows data for the healthy controls and patients with liver diseases. The compound concentration in each individual was divided by the average concentration in the healthy controls and the obtained values were then averaged again for each disease. The metabolites highlighted in blue showed large fold changes (disease/control ratios of >2.5) in an average of seven liver diseases. *p <0.05, **p <0.01, ***p <0.0001, significance difference by the Kruskal–Wallis test. The compounds were clustered based on elucidation distances. Red and green denote relatively high and low concentrations, respectively, compared with the average concentration.

weights with those of the standards. Significant differences were observed among controls and liver diseases (p <0.0001; Kruskal–Wallis test) except for γ-Glu-Met in the validation data (Supplementary Tables 1 and 2). Correlational cluster analyses of 67 compounds showed that all the γ-glutamyl dipeptides except for γ-Glu-Tyr and γ-Glu-Trp were clustered with AST, ALT, and metabolites involved in oxidative stress responses, namely glucosamine [16] and methionine sulfoxide [17–19] (Fig. 1).

Statistical analysis and validation for biomarker discovery

From the serum samples obtained at YUH, we selected 89 liver disease patients including DI, AHB, CHB, CNALT, CHC, CIR, and HCC patients, and 53 healthy controls with no significant differences in the age distribution between the training and validation cohorts (Table 1). As shown in the whisker box plots for the training cohort (Fig. 2), the levels of γ-glutamyl dipeptides and of AST and ALT, as commonly used hepatocyte biomarkers, were increased in different patterns in comparison with C. For example, the AST and ALT levels were significantly increased in patients with DI, CHB, CHC, CIR, and HCC (p <0.05; Dunn's post-test), but not in those with AHB and CNALT (Fig. 2). On the other hand, significant increases were observed in the levels of γ-Glu-Ser, γ-Glu-Val, γ-Glu-Thr, γ-Glu-Leu, and γ-Glu-Phe (p <0.05; Dunn's post-test) in AHB and in the levels of all the γ-glutamyl derivatives of amino acids (p <0.05; Dunn's post-test) except for ophthalmate, γ-Glu-Thr, and γ-Glu-Trp in CNALT (Fig. 2 and Supplementary Table 1). Oxidative metabolites, methionine sulfoxide, and glucosamine were significantly increased in all diseases (p <0.05; Dunn's post-test) and in CHB, CNALT, and CHC (p <0.0001; Dunn's post-test), respectively (Fig. 2).

To assess their abilities to discriminate specific liver diseases from other liver diseases, we developed MLR models using combinations of several components of the γ-glutamyl dipeptides, transaminases, and oxidative metabolites using the training dataset. For example, an MLR model incorporating four selected biomarkers (γ-Glu-Ala, γ-Glu-Citrulline, γ-Glu-Thr, and γ-Glu-Phe) was able to differentiate HCC from the other groups (C, DI, AHB, CHB, CNALT, CHC, and CIR) with an area under the receiver-operating characteristic (ROC) curve (AUC) value of 0.762 (95% CI 0.647–0.877, p = 0.00025). The probability (p) of HCC is calculated by: $\log(p/(1-p)) = -1.87 - 1.13 \times$ γ-Glu-Ala $+ 3.51 \times$ γ-Glu-Citrulline $- 1.65 \times$ γ-Glu-Thr $+ 6.99 \times$ γ-Glu-Phe (Table 2). When the concentrations of γ-Glu-Ala, γ-Glu-Citrulline, γ-Glu-Thr, and γ-Glu-Phe are 1.7, 0.84, 0.54, and 0.34 μM, respectively, the probability of HCC is 65.5%. All the MLR models achieved high AUC values at statistically significant levels (between 0.754 and 0.972, p <0.011) (Fig. 3, Table 2 and Supplementary Table 3).

The developed MLR models were evaluated in a blinded manner using an independent cohort (YUH) consisting of 75 individuals who were not members of the training cohort (Supplementary Table 2). We found that all of the MLR models also produced high AUC values at statistically significant levels (between 0.707 and 0.993, p <0.023) (Fig. 3, Table 2 and Supplementary Table 3). Although C, CHB, and CHC were each differentiated from the other groups by a single γ-glutamyl dipeptide (γ-Glu-Phe, γ-Glu-Thr, and γ-Glu-Lys, respectively), the MLR models for the other diseases required multiple biomarkers to achieve accurate discrimination (Table 2). The odds ratios of ALT, AST, and methionine sulfoxide were close to 1.0 compared with the odds ratios of the γ-glutamyl dipeptides, indicating their

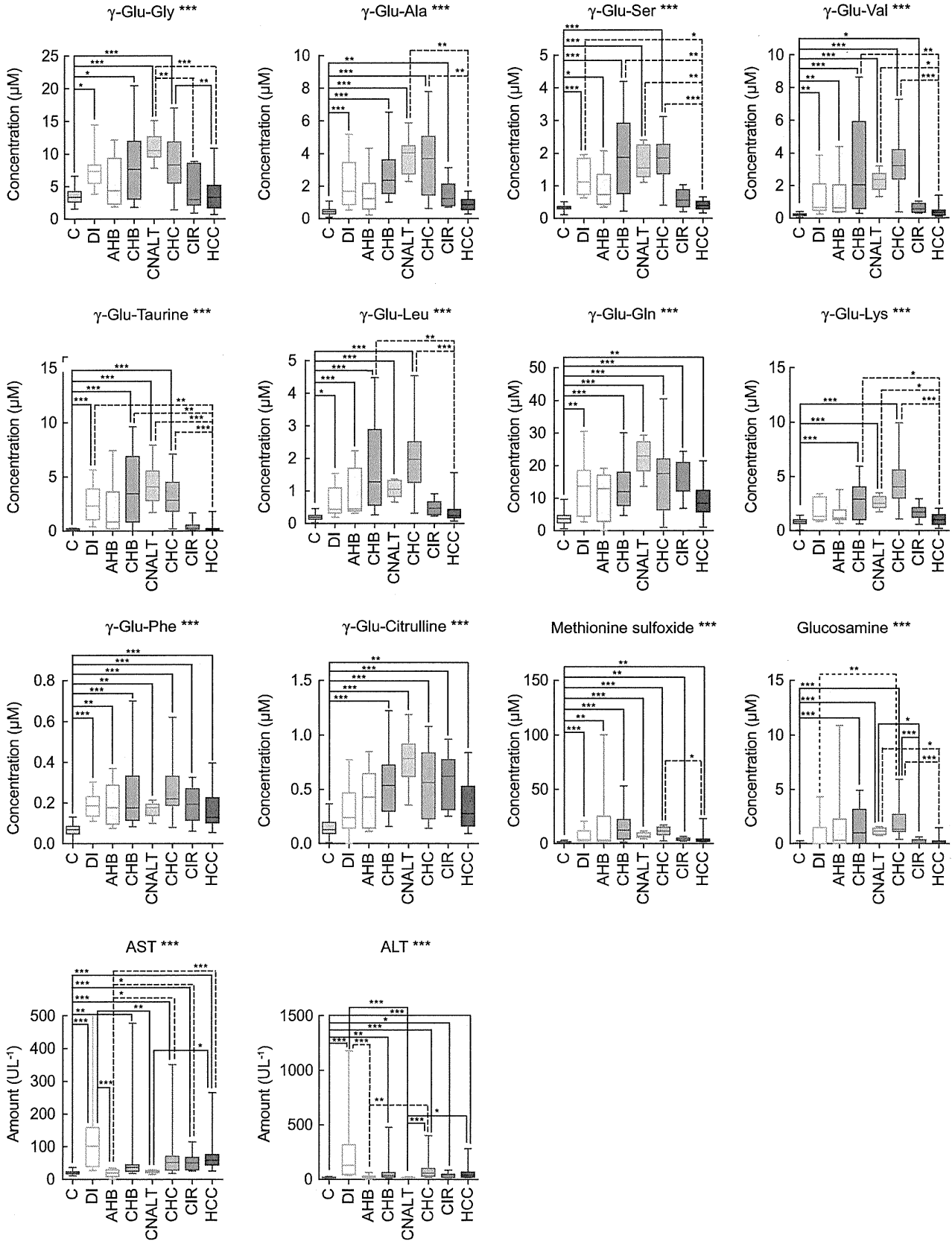
γ-Glu-Gly ***
γ-Glu-Ala ***
γ-Glu-Ser ***
γ-Glu-Val ***
γ-Glu-Taurine ***
γ-Glu-Leu ***
γ-Glu-Gln ***
γ-Glu-Lys ***
γ-Glu-Phe ***
γ-Glu-Citrulline ***
Methionine sulfoxide ***
Glucosamine ***
AST ***
ALT ***
Concentration (μM)
Amount (UL-1)
C
DI
AHB
CHB
CNALT
CHC
CIR
HCC

Table 2. Biomarkers for discriminating each liver disease selected by MLR models.

Group	Biomarker	Coefficient	95% CI		Odds ratio	95% CI		*p* value
C	(Intercept)	5.77	3.84	8.32	—	—	—	<0.0001
	γ-Glu-Phe	-58.2	-84.3	-39.0	5.16×10^{-26}	2.47×10^{-37}	1.15×10^{-17}	<0.0001
DI	(Intercept)	-3.08	-4.49	-1.94	—	—	—	<0.0001
	ALT	0.020	7.89×10^{-3}	0.034	1.02	1.01	1.03	2.00×10^{-3}
	γ-Glu-Citrulline	-1.55	-5.01	1.13	0.21	6.68×10^{-3}	3.11	0.31
AHB	(Intercept)	-1.52	-3.35	0.63	—	—	—	0.12
	AST	-0.057	-0.15	-4.96×10^{-3}	0.94	0.86	1.00	0.12
	Methionine sulfoxide	0.072	0.018	0.15	1.08	1.02	1.17	0.047
CHB	(Intercept)	-4.52	-6.33	-3.24	—	—	—	<0.0001
	γ-Glu-Thr	1.52	0.65	2.63	4.58	1.91	13.9	2.30×10^{-3}
CNALT	(Intercept)	-0.76	-3.15	1.94	—	—	—	0.55
	ALT	-0.16	-0.34	-0.049	0.85	0.71	0.95	0.032
	γ-Glu-Taurine	0.80	0.43	1.31	2.23	1.54	3.72	3.00×10^{-4}
CHC	(Intercept)	-4.73	-6.39	-3.47	—	—	—	<0.0001
	γ-Glu-Lys	1.27	0.85	1.82	3.57	2.34	6.14	<0.0001
CIR	(Intercept)	-2.79	-4.05	-1.55	—	—	—	<0.0001
	γ-Glu-Ala	1.80	0.42	3.52	6.05	1.52	33.7	0.020
	γ-Glu-Leu	-0.066	-3.06	2.24	0.94	0.047	9.42	0.96
	γ-Glu-Ser	-1.35	-5.35	1.86	0.26	4.77×10^{-3}	6.44	0.41
	γ-Glu-Taurine	-2.28	-5.07	-0.33	0.10	6.27×10^{-3}	0.72	0.064
HCC	(Intercept)	-1.87	-2.90	-0.90	—	—	—	2.00×10^{-4}
	γ-Glu-Ala	-1.13	-2.44	-0.14	0.32	0.087	0.87	0.050
	γ-Glu-Citrulline	3.51	0.45	7.00	33.4	1.57	1.10×10^{3}	0.033
	γ-Glu-Thr	-1.65	-5.12	0.49	0.19	5.95×10^{-3}	1.63	0.27
	γ-Glu-Phe	6.99	-0.52	14.7	1.09×10^{3}	5.92×10^{-1}	2.50×10^{6}	0.063

Note: The en-dashes in the 95% CI columns indicate that these values could not be calculated. Biomarker and coefficients are used in MLR model to calculate the probability of each disease. Intercept indicates the constant term in MLR models.

relatively lower contributions to the separation ability of the MLR models (Table 2). Overall, for all types of liver diseases, the MLR models mostly based on γ-glutamyl dipeptides provided complementary results, even in the second (validation) cohort.

γ-Glutamyl dipeptides as biomarkers for HCC and NAFLD

To evaluate the diagnostic potential of γ-glutamyl dipeptides for HCC, we compared their diagnostic abilities with that of AFP, an established marker for HCC (Fig. 4). We found that the MLR models using four γ-glutamyl dipeptides (γ-Glu-Ala, γ-Glu-Citrulline, γ-Glu-Thr, γ-Glu-Phe) (Table 2) were better at distinguishing HCC from CHC and CIR (AUC = 0.881) than AFP (AUC = 0.760) (Fig. 4).

We further investigated the biomarker specificities by comparing the serum γ-glutamyl dipeptide levels in GC and HCC patients (Supplementary Fig. 2 and Table 4). The analyses revealed significant differences, with the exception of γ-Glu-Phe, and the levels of γ-glutamyl dipeptides were notably low in GC.

Differences in the levels of γ-glutamyl dipeptides were also observed in NAFLD. The levels of six γ-glutamyl dipeptides (γ-Glu-Val, γ-Glu-Thr, γ-Glu-Leu, γ-Glu-His, γ-Glu-Phe, and γ-Glu-Arg) were significantly higher ($p < 0.05$; Mann–Whitney test) in SS than in NASH (Supplementary Fig. 3 and Table 5). Although further investigations are necessary, these dipeptides can be used as noninvasive biomarkers in rapid screening for SS and NASH.

Mechanism of γ-glutamyl dipeptide biosynthesis

To confirm the γ-glutamyl dipeptide biosynthesis pathway, the hepatic metabolism was investigated using a mouse model. In

Fig. 2. Representative whisker box plots of the serum levels of detected transaminases and metabolites in the training cohort. The horizontal lines indicate the upper median, median, and lower median, and the whiskers show the maximum and minimum levels. One plot for AST was outside the range (>500 U/L). *$p < 0.05$, **$p < 0.01$, ***$p < 0.0001$, significance difference by the Kruskal–Wallis test and Dunn's post-test for each marker and two groups in each marker, respectively.

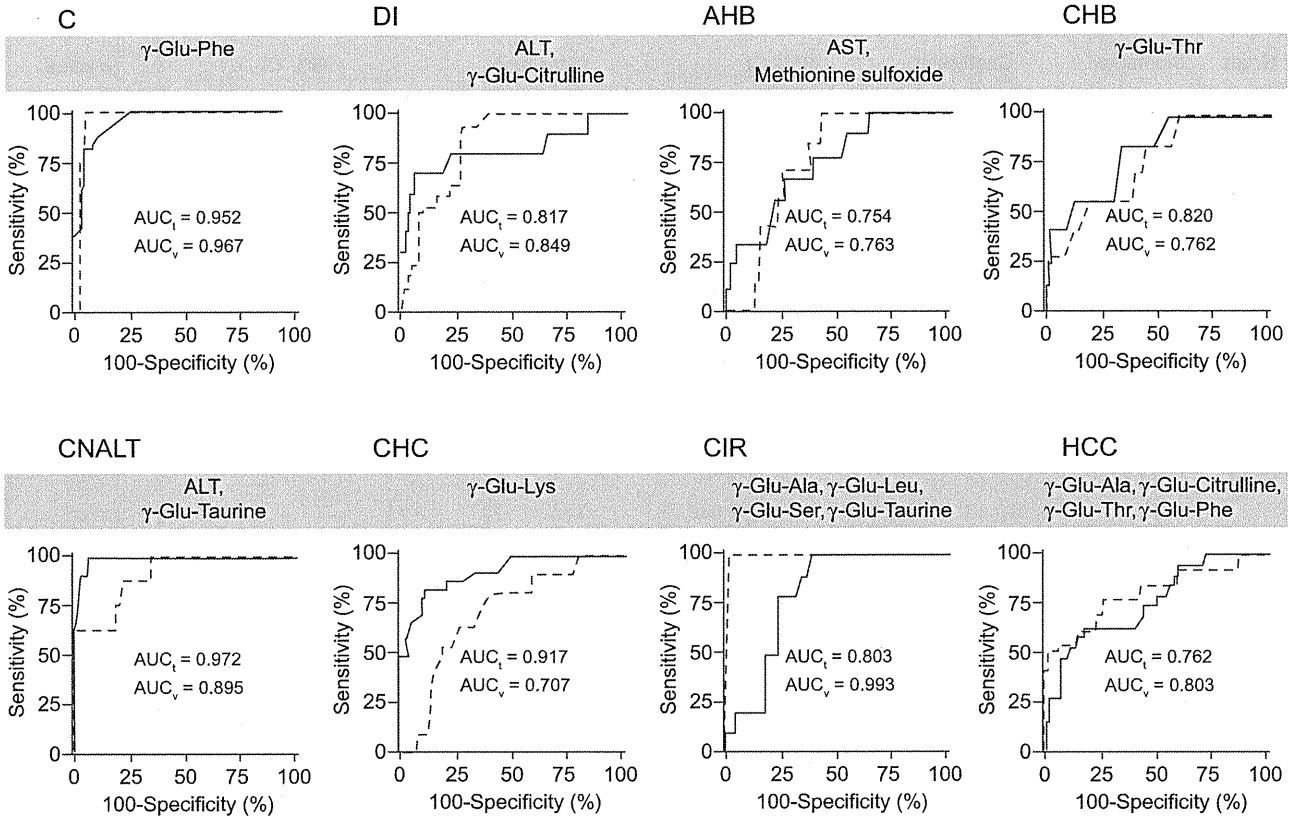

Fig. 3. ROC curve analyses of the ability of γ-glutamyl peptides alone or in combination with AST, ALT and methionine sulfoxide to discriminate each group from all other liver diseases and healthy controls. The solid and dashed curves represent the ROC curves for the training and validation cohorts, respectively. AUCt and AUCv in each panel indicate the AUC values in the training and validation cohorts, respectively. The group label indicates the discriminated group from all the other groups by an MLR model. The biomarkers in each panel were used in the MLR model for discriminating the group, e.g., ALT and γ-Glu-Taurine were the biomarkers for discriminating CNALT from the other groups. The coefficients and constant term of the MLR model of these biomarkers were summarized in Table 2.

acetaminophen (APAP)-treated mice [12], ophthalmate, a γ-glutamyl tripeptide, was synthesized through consecutive reactions with GCS and glutathione synthetase (GS), the same enzymes that play a role in GSH synthesis [12] (Fig. 5). Therefore, we investigated the alterations in the levels of hepatic amino acids, amines, γ-glutamyl dipeptides, and tripeptides after administration of buthionine sulfoximine (BSO), diethylmaleate (DEM) or APAP (Supplementary Fig. 4). BSO treatment resulted in GCS inhibition [20] and marked reductions in most of the hepatic γ-glutamyl dipeptide and tripeptide levels (Fig. 5 and Supplementary Fig. 4A). In contrast, DEM treatment led to GSH depletion by oxidation of the thiol group in GSH [21], resulting in GCS activation and considerable increases in the hepatic γ-glutamyl dipeptide and tripeptide levels compared with the controls (Fig. 5 and Supplementary Fig. 4A). The hepatic levels of several γ-glutamyl dipeptides and tripeptides were increased with concurrent GSH depletion in APAP-treated mice (Supplementary Fig. 4B and C). These results indicated that in mice, γ-glutamyl dipeptides and tripeptides were certainly synthesized via the ligation of glutamate by various amino acids through consecutive reactions with GCS and GS when GSH was depleted (Fig. 5). The identification details for the γ-glutamyl dipeptide biosynthetic pathway are described in the Supplementary data.

Discussion

Our analyses of 237 serum samples from patients with liver diseases and healthy controls revealed that γ-glutamyl dipeptides were increased in liver injuries and could provide specific information for different liver diseases. In APAP-induced liver injury in mice, ophthalmate, a γ-glutamyl tripeptide, was markedly increased as a byproduct of GSH synthesis [21] (Fig. 5 and Supplementary Fig. 4B). However, in liver diseases in humans, many γ-glutamyl dipeptides were primarily synthesized and secreted from hepatocytes into the blood (Figs. 1 and 5). Although the reason for the difference is unclear, it may be attributable to species differences in the levels and activities of enzymes and transporters [22,23].

In all types of liver disease, oxidative stress resulting from an imbalance between the production of reactive oxygen species (ROS) and the ability of a biological system to detoxify reactive intermediates plays a crucial role in the induction and progression of liver damage independently of its etiology [1]. In patients with hepatitis, oxidative stress is produced by inflammation induced by immunological mechanisms. Upon viral infection, NADPH oxidase produces ROS in neutrophils and macrophages, and ROS are also generated from free iron through the Fenton reaction [24–26]. ROS are further produced in hepatocytes upon

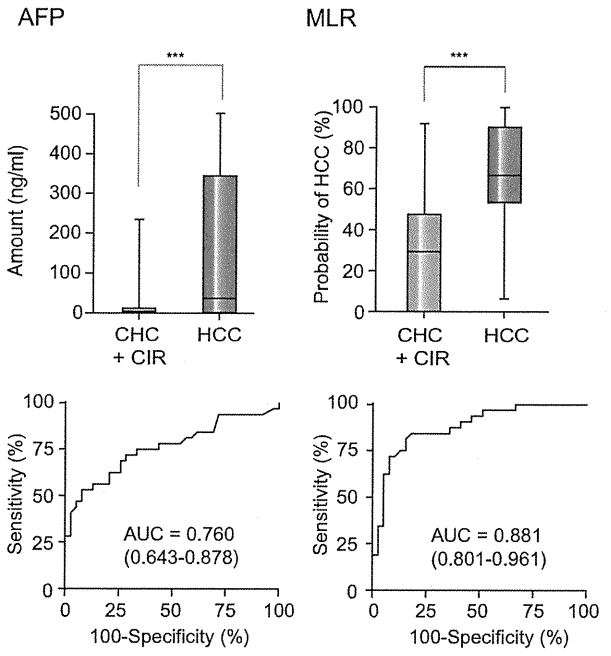

Fig. 4. Whisker box plots and ROC curves of AFP and MLR analyses based on γ-Glu-Ala, γ-Glu-Citrulline, γ-Glu-Thr and γ-Glu-Phe for discriminating patients with HCC (n = 32) from patients with CHC (n = 35) and CIR (n = 18).

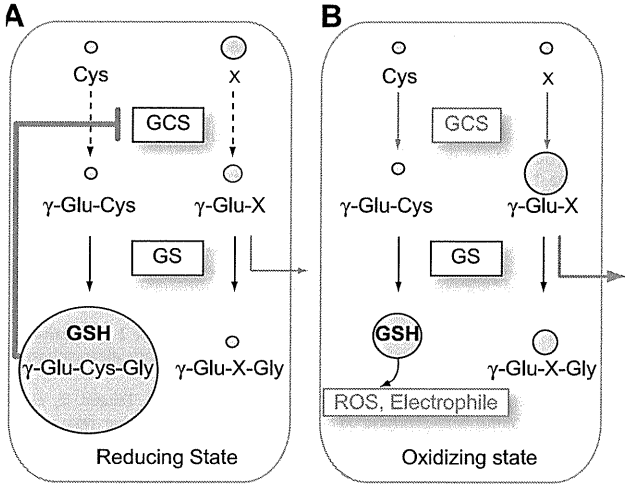

Fig. 5. Biosynthetic mechanism of γ-glutamyl peptides in hepatocytes under (A) reducing conditions and (B) oxidative stress. GCS is feedback-inhibited by GSH under reducing conditions and small amounts of γ-glutamyl dipeptides are synthesized. During oxidative stress, GSH is consumed, leading to GCS activation. This could result in biosynthesis of γ-glutamyl dipeptides, which are then effluxed across the hepatocellular membrane. γ-Glutamyl dipeptides and tripeptides are indicated by γ-Glu-X and Glu-X-Gly, respectively (X = amino acid or amine).

the release of inflammatory cytokines, such as tumor necrosis factor-α and interleukin-1β from inflammatory cells [27]. GSH is the most abundant antioxidant in hepatocytes, and helps to protect cells against ROS. Upon depletion of GSH, ROS induce oxidative stress resulting in liver damage, and reduced GSH levels have been demonstrated in various liver diseases [28–30].

Since γ-glutamyl dipeptides are byproducts of GSH synthesis catalyzed by GCS, their levels are indirect evidence for GSH production (Fig. 5). Different levels of γ-glutamyl dipeptides were observed in different types of liver disease and each γ-glutamyl dipeptide showed a somewhat different variation pattern among liver diseases (Fig. 2). This might be attributed to differences in hepatic levels of amino acids (the substrate of GCS) among liver diseases, though further studies are necessary to understand the details of this observation.

In healthy controls, the γ-glutamyl dipeptide levels were low. This occurred because under reducing conditions, the level of hepatic GSH was high and a small amount of GSH was biosynthesized (Fig. 5A). However, in the patients with liver diseases, GSH was consumed to neutralize the generated ROS, which in turn led to GCS activation, resulting in the biosynthesis of GSH together with γ-glutamyl dipeptides (Fig. 5B). Therefore, increased levels of γ-glutamyl dipeptides were observed in most liver injuries. Surprisingly, unlike AST and ALT, the levels of most γ-glutamyl dipeptides were markedly increased in asymptomatic individuals with AHB and CNALT (Fig. 2 and Supplementary Fig. 1), possibly because viral infection induced ROS generation followed by GSH depletion, which led to the biosynthesis of GSH and γ-glutamyl dipeptides (Fig. 5). We hypothesize that sufficiently high levels of GSH production neutralized ROS, resulting in lower incidences of AHB and CNALT.

There are relationships between liver diseases attributable to HCV infection and oxidative stress parameters, such as ROS, antioxidants, and inflammation. Oxidative stress increased with hepatic disease progression in HCV-infected patients [31]. Consistent with that report, among all the patients with HCV-related liver diseases, the serum levels of γ-glutamyl dipeptides, as indicators of hepatic GSH production, were markedly increased in CNALT and tended to decrease with disease progression (CNALT ⩾ CHC > CIR > HCC) (Fig. 2). These observations led us to conclude that at the time of viral infection (CNALT), a sufficient amount of GSH production can neutralize ROS and thus weaken the pathogenesis of liver damage. However, when GSH production falls below ROS generation, oxidative stress followed by inflammation is induced, resulting in the development and progression of liver diseases. Similarly, the levels of several γ-glutamyl dipeptides were significantly lower in NASH patients than in SS patients (Supplementary Fig. 3), indicating low levels of GSH production in NASH patients. Based on the present observations, we suggest that NASH is susceptible to oxidative stress and progression to liver fibrosis and cirrhosis.

HCC is one of the most common cancers in humans, and primarily develops in patients with chronic liver disease. Its early detection is important because effective treatments are available for the management of non-advanced cancers [32]. Until now, the diagnosis of HCC has relied on combinations of imaging techniques and measurements of the serum levels of AFP [33] and PIVKA-II [34]. Although they are reliable tumor markers for the diagnosis and monitoring of primary HCC, high levels of serum AFP and plasma PIVKA-II have also been observed in some gastric carcinomas [34,35]. However, the serum γ-glutamyl dipeptide levels in GC and HCC patients revealed significant differences, and the levels of several γ-glutamyl dipeptides was notably low in GC (Supplementary Fig. 2). We suspect that this occurred through differences in the tissue activities of the glutathione

system, since GSH is mainly synthesized *de novo* in the liver, and hypothesize that the γ-glutamyl dipeptide levels may reflect hepatic dysfunction.

Drug-induced hepatotoxicity is a frequent cause of liver injury, and the predominant clinical presentation is acute hepatitis and/or cholestasis. Overdoses of APAP, the most commonly used analgesic and antipyretic, can lead to possibly fatal hepatitis and several hundred deaths attributable to this drug occur annually in the United States. Our DI samples were from patients with so-called idiosyncratic hepatotoxicity, and the underlying mechanisms of this disease remain unclear. Interestingly, the changes in the serum levels of γ-glutamyl dipeptides were similar among the DI samples although the causative drugs differed widely and the mechanisms responsible for the development of hepatotoxicity may also be different. Our findings revealed that the amount of γ-glutamyl dipeptide production attributable to a reduction in the hepatocellular GSH concentration was a common feature in drug-induced idiosyncratic hepatotoxicity. With AUC values of 0.817 (training data) and 0.849 (validation data) (Supplementary Table 3), the serum levels of ALT and γ-Glu-Citrulline could be used to distinguish between DI patients on the one hand and patients with viral hepatitis infection and healthy controls on the other (Table 2). Therefore, we suggest that these compounds represent noninvasive biomarkers that facilitate rapid screening for DI.

In summary, our CE–TOFMS and LC–MS/MS metabolomics-based analyses of serum samples from patients with liver diseases showed quantitative differences in γ-glutamyl dipeptides in various liver diseases. Our highly specific set of γ-glutamyl dipeptides, transaminases, and methionine sulfoxide enabled us to discriminate among liver diseases including DI, AHB, CHB, CNALT, CHC, CIR, and HCC, indicating that they can be used as multiple biomarkers in rapid screening for different types and stages of liver disease. Furthermore, we have shown that γ-glutamyl dipeptide synthesis was catalyzed by GCS, the enzyme that is feedback-inhibited by GSH, and thus the levels of these biomarkers were indicative of hepatic GSH production. As observed in patients with HCV-related liver diseases and NAFLD, the serum γ-glutamyl dipeptide levels tended to decrease during the course of liver disease progression, indicating an increase in oxidative stress resulting from decreased GSH production during liver disease progression. Therefore, γ-glutamyl dipeptide measurement can potentially provide valuable information about the hepatic reduction–oxidation state to gain insights into the role of oxidative stress in the pathogenesis and progression of liver diseases.

Conflict of interest

The Authors who have taken part in this study declared that they do not have anything to disclose regarding funding or conflict of interest with respect to this manuscript.

Financial support

This work was supported by Health and Labour Sciences Research Grants "Research on Biological Markers for New Drug Development" (T.S.) and "Research on Risk of Chemical Substances" (T.S.). Additional support was obtained through grants from the Ministry of Education, Culture, Sports, Science and Technology (MEXT) for a Global COE Program entitled "Human Metabolomic Systems Biology" in Life Sciences (T.S., M.T. and M.S.) and the ERATO Gas Biology Project (M.S.), as well as research funds from the Yamagata Prefectural Government and City of Tsuruoka.

Supplementary data

Supplementary data associated with this article can be found, in the online version, at doi:10.1016/j.jhep.2011.01.031.

References

[1] Loguercio C, Federico A. Oxidative stress in viral and alcoholic hepatitis. Free Radic Biol Med 2003;34:1–10.
[2] Brunt EM. Nonalcoholic steatohepatitis. Semin Liver Dis 2004;24:3–20.
[3] Younossi ZM, Jarrar M, Nugent C, Randhawa M, Afendy M, Stepanova M, et al. A novel diagnostic biomarker panel for obesity-related nonalcoholic steatohepatitis (NASH). Obes Surg 2008;18:1430–1437.
[4] Piccinino F, Sagnelli E, Pasquale G, Giusti G. Complications following percutaneous liver biopsy. A multicentre retrospective study on 68,276 biopsies. J Hepatol 1986;2:165–173.
[5] Bolukbas C, Bolukbas FF, Horoz M, Aslan M, Celik H, Erel O. Increased oxidative stress associated with the severity of the liver disease in various forms of hepatitis B virus infection. BMC Infect Dis 2005;5:95.
[6] Sreekumar A, Poisson LM, Rajendiran TM, Khan AP, Cao Q, Yu J, et al. Metabolomic profiles delineate potential role for sarcosine in prostate cancer progression. Nature 2009;457:910–914.
[7] Bogdanov M, Matson WR, Wang L, Matson T, Saunders-Pullman R, Bressman SS, et al. Metabolomic profiling to develop blood biomarkers for Parkinson's disease. Brain 2008;131:389–396.
[8] Wang C, Kong H, Guan Y, Yang J, Gu J, Yang S, et al. Plasma phospholipid metabolic profiling and biomarkers of type 2 diabetes mellitus based on high-performance liquid chromatography/electrospray mass spectrometry and multivariate statistical analysis. Anal Chem 2005;77:4108–4116.
[9] Sabatine MS, Liu E, Morrow DA, Heller E, McCarroll R, Wiegand R, et al. Metabolomic identification of novel biomarkers of myocardial ischemia. Circulation 2005;112:3868–3875.
[10] Kenny LC, Dunn WB, Ellis DI, Myers J, Baker PN, Consortium TG, et al. Novel biomarkers for pre-eclampsia detected using metabolomics and machine learning. Metabolomics 2005;1:227–234.
[11] Soga T, Ohashi Y, Ueno Y, Naraoka H, Tomita M, Nishioka T. Quantitative metabolome analysis using capillary electrophoresis mass spectrometry. J Proteome Res 2003;2:488–494.
[12] Soga T, Baran R, Suematsu M, Ueno Y, Ikeda S, Sakurakawa T, et al. Differential metabolomics reveals ophthalmic acid as an oxidative stress biomarker indicating hepatic glutathione consumption. J Biol Chem 2006;281:16768–16776.
[13] Soga T, Igarashi K, Ito C, Mizobuchi K, Zimmermann HP, Tomita M. Metabolomic profiling of anionic metabolites by capillary electrophoresis mass spectrometry. Anal Chem 2009;81:6165–6174.
[14] Shintani T, Iwabuchi T, Soga T, Kato Y, Yamamoto T, Takano N, et al. Cystathionine beta-synthase as a carbon monoxide-sensitive regulator of bile excretion. Hepatology 2009;49:141–150.
[15] Goto S, Okuno Y, Hattori M, Nishioka T, Kanehisa M. LIGAND: database of chemical compounds and reactions in biological pathways. Nucleic Acids Res 2002;30:402–404.
[16] Kaneto H, Xu G, Song KH, Suzuma K, Bonner-Weir S, Sharma A, et al. Activation of the hexosamine pathway leads to deterioration of pancreatic beta-cell function through the induction of oxidative stress. J Biol Chem 2001;276:31099–31104.
[17] Levine RL, Berlett BS, Moskovitz J, Mosoni L, Stadtman ER. Methionine residues may protect proteins from critical oxidative damage. Mech Ageing Dev 1999;107:323–332.
[18] Babior BM. Phagocytes and oxidative stress. Am J Med 2000;109:33–44.
[19] Vogt W. Oxidation of methionyl residues in proteins: tools, targets, and reversal. Free Radic Biol Med 1995;18:93–105.
[20] Griffith OW, Meister A. Potent and specific inhibition of glutathione synthesis by buthionine sulfoximine (*S-n*-butyl homocysteine sulfoximine). J Biol Chem 1979;254:7558–7560.
[21] Zalups RK, Lash LH. Depletion of glutathione in the kidney and the renal disposition of administered inorganic mercury. Drug Metab Dispos 1997;25:516–523.

[22] Ishizuka H, Konno K, Shiina T, Naganuma H, Nishimura K, Ito K, et al. Species differences in the transport activity for organic anions across the bile canalicular membrane. J Pharmacol Exp Ther 1999;290:1324–1330.
[23] Mainwaring GW, Williams SM, Foster JR, Tugwood J, Green T. The distribution of theta-class glutathione *S*-transferases in the liver and lung of mouse, rat and human. Biochem J 1996;318:297–303.
[24] Marrogi AJ, Khan MA, van Gijssel HE, Welsh JA, Rahim H, Demetris AJ, et al. Oxidative stress and p53 mutations in the carcinogenesis of iron overload-associated hepatocellular carcinoma. J Natl Cancer Inst 2001;93:1652–1655.
[25] Toyokuni S, Okamoto K, Yodoi J, Hiai H. Persistent oxidative stress in cancer. FEBS Lett 1995;358:1–3.
[26] Sutton A, Nahon P, Pessayre D, Rufat P, Poire A, Ziol M, et al. Genetic polymorphisms in antioxidant enzymes modulate hepatic iron accumulation and hepatocellular carcinoma development in patients with alcohol-induced cirrhosis. Cancer Res 2006;66:2844–2852.
[27] Koike K, Miyoshi H. Oxidative stress and hepatitis C viral infection. Hepatol Res 2006;34:65–73.
[28] Boya P, de la Pena A, Beloqui O, Larrea E, Conchillo M, Castelruiz Y, et al. Antioxidant status and glutathione metabolism in peripheral blood mononuclear cells from patients with chronic hepatitis C. J Hepatol 1999;31:808–814.
[29] Tanyalcin T, Taskiran D, Topalak O, Batur Y, Kutay F. The effects of chronic hepatitis C and B virus infections on liver reduced and oxidized glutathione concentrations. Hepatol Res 2000;18:104–109.
[30] Moriya K, Nakagawa K, Santa T, Shintani Y, Fujie H, Miyoshi H, et al. Oxidative stress in the absence of inflammation in a mouse model for hepatitis C virus-associated hepatocarcinogenesis. Cancer Res 2001;61:4365–4370.
[31] Sumida Y, Nakashima T, Yoh T, Nakajima Y, Ishikawa H, Mitsuyoshi H, et al. Serum thioredoxin levels as an indicator of oxidative stress in patients with hepatitis C virus infection. J Hepatol 2000;33:616–622.
[32] Bruix J. Treatment of hepatocellular carcinoma. Hepatology 1997;25:259–262.
[33] Szklaruk J, Silverman PM, Charnsangavej C. Imaging in the diagnosis, staging, treatment, and surveillance of hepatocellular carcinoma. Am J Roentgenol 2003;180:441–454.
[34] Kudo M, Takamine Y, Nakamura K, Shirane H, Uchida H, Kasakura S, et al. Des-gamma-carboxy prothrombin (PIVKA-II) and alpha-fetoprotein-producing IIc-type early gastric cancer. Am J Gastroenterol 1992;87:1859–1862.
[35] Takano S, Honda I, Watanabe S, Soda H, Nagata M, Hoshino I, et al. PIVKA-II-producing advanced gastric cancer. Int J Clin Oncol 2004;9:330–333.

STEM CELLS AND DEVELOPMENT
Volume 20, Number 9, 2011

DOI: 10.1089/scd.2011.0074

Potential Therapeutic Application of Intravenous Autologous Bone Marrow Infusion in Patients with Alcoholic Liver Cirrhosis

Takafumi Saito,[1] Kazuo Okumoto,[1] Hiroaki Haga,[1] Yuko Nishise,[1] Rika Ishii,[1] Chikako Sato,[1] Hisayoshi Watanabe,[1] Akio Okada,[2] Motoki Ikeda,[2] Hitoshi Togashi,[3] Tsuyoshi Ishikawa,[4] Shuji Terai,[4] Isao Sakaida,[4] and Sumio Kawata[1]

The present study was conducted to evaluate the application and efficacy of autologous bone marrow infusion (ABMi) for improvement of liver function in patients with alcoholic liver cirrhosis (ALC). Five subjects and 5 control patients with ALC who had abstained from alcohol intake for 24 weeks before the study were enrolled. Autologous bone marrow cells were washed and injected intravenously, and the changes in serum liver function parameters, and the level of the type IV collagen 7S domain as a marker of fibrosis, were monitored for 24 weeks. The distribution of activated bone marrow was assessed by indium-111-chloride bone marrow scintigraphy. The number of cells infused was $8.0 \pm 7.3 \times 10^9$ (mean ± standard error). The serum levels of albumin and total protein and the prothrombin time were significantly higher during the follow-up period after ABMi than during the observation period in treated patients, whereas no such changes were observed in the controls. In the patients who received ABMi, the Child-Pugh score decreased in all 3 who were classified as class B; the serum levels of type IV collagen 7S domain improved in 4 of the 5 patients; and bone marrow scintigraphy demonstrated an increase of indium-111-chloride uptake in 3 of the 4 patients tested. ABMi for patients with ALC helps improve liver function parameters in comparison with observation during abstinence and ameliorates the degree of fibrosis in terms of serum markers and bone marrow activation in most cases.

Introduction

Liver cirrhosis is the end stage of chronic liver disease, and it is associated with many serious systemic complications resulting from both liver failure and portal hypertension. This condition has a poor prognosis and is difficult to treat. Liver transplantation is the only curative remedy, but it is associated with many problems such as donor shortage, surgical complications, rejection, and high cost. As an alternative approach, regenerative cell therapy using stem cells is now being investigated. In particular, multipotent stem cells present in bone marrow (BM) are a promising candidate for this purpose, and clinical trials aiming at therapy of cardiovascular diseases have been performed [1,2].

BM cells have been shown to be capable of differentiating into the liver cell lineage, and transplantation of BM cells has considerable potential for regeneration of liver tissue [3–6]. The degree of liver function and fibrosis as well as survival rate have been shown to improve significantly as a result of BM cell transplantation in animal models of severe liver injury [7,8]. We have experimentally investigated the potential of BM stem cells to differentiate into the hepatocyte lineage both in vitro or in vivo with a view to possible application for clinical trials aimed at liver regeneration [9–12]. In this context, the effectiveness of CD34+ hematopoietic stem cell injection into the liver via the portal vein or hepatic artery had been shown to improve the serum levels of albumin and bilirubin [13,14]. Our research group has already reported the therapeutic effectiveness of whole-BM peripheral infusion, referred to as autologous BM cell infusion (ABMi) therapy for patients with cirrhosis with hepatitis B or C [15,16].

Alcoholic liver injury is a common liver disease worldwide. Although disease activity may be decreased by abstinence in the initial phase, it eventually progresses to cirrhosis and finally to death unless patients receive appropriate therapeutic intervention for both liver injury and alcohol abuse. Even if patients discontinue alcohol intake, those in whom the disease has progressed to advanced cirrhosis with marked liver fibrosis have a poor prognosis because of

Departments of [1]Gastroenterology and [2]Radiology, Yamagata University School of Medicine, Yamagata, Japan.
[3]Health Administrative Center, Yamagata University, Yamagata, Japan.
[4]Department of Gastroenterology and Hepatology, Yamaguchi University Graduate School of Medicine, Ube, Yamaguchi, Japan.

serious complications and liver cell dysfunction. Therefore, such patients require some form of liver-regenerative therapy, as well as abstinence, to improve the liver function. Since such patients are free of pathogens such as hepatitis B or hepatitis C that cause continuous liver necroinflammation, ABMi might facilitate a degree of liver regeneration if abstinence is maintained along with appropriate nutritional care. Pai et al. reported that autologous infusion of expanded mobilized BM-derived CD34+ cells into patients with alcoholic liver cirrhosis (ALC) via the hepatic artery improved the serum levels of both bilirubin and transaminase, as well as the Child-Pugh score [17].

To investigate the effectiveness of ABMi for patients with ALC, we applied it to such patients and examined the resulting changes in liver function parameters. In addition, using indium-111-chloride (^{111}In) BM scintigraphy, we tracked the infused BM cells after ABMi.

Patients and Methods

Patients

Patients with a diagnosis of advanced liver cirrhosis due to alcoholic liver injury were enrolled. All the patients were negative for both anti-hepatitis C virus antibody and hepatitis B surface antigen and had a history of excessive alcohol consumption exceeding 60 g/day of ethanol for >5 years. The patients were interviewed, and those who had abstained for >24 weeks before the interview were entered into the study. The inclusion criteria for clinical parameters were as follows: platelet count >50,000/mm^3, total bilirubin <3 mg/dL, and absence of liver cancer on computed tomography (CT). Both heart and lung function were screened to confirm whether general anesthesia was possible. As a control group, we used patients who were not given ABMi, but who agreed to the use of their clinical data for study. Those patients had also been diagnosed as having ALC, and were matched to the subjects who received ABMi for age, sex, medication, and various biochemical parameters; their liver function parameters were compared with those of the subjects who received ABMi during the study period.

Autologous BM cell preparation and infusion into patients

A total of 400 mL BM was harvested from the ilium according to the standard procedure under general anesthesia and collected in a plastic bag containing heparin. After fat had been removed from the top of the bag, hydroxyethyl starch was added to a final concentration of 1%. Red blood cells were precipitated after 40 min of incubation at room temperature. We used an automated bench-top device (Cytomate; Takara Bio Inc., Otsu, Shiga, Japan), which is a functionally closed system incorporating a spinning membrane connected to a filter wash bag, for washing and concentrating the mononuclear cells (MNCs). The final cell products were washed, concentrated, and made up to a final volume of 105 mL. Five milliliters of the final cell product was subjected to the trypan blue dye exclusion test, endotoxin test, and fluorescence-activated cell sorting analysis. CD34+, CD44+, CD45+, and CD117+ cells were determined by flow cytometry at the central laboratory of SRL Inc., Tokyo, Japan. At 6 h after BM harvest, the final MNCs preparation was administered to each patient via the cubital vein by drip infusion. All the study protocols were approved by the ethics committee of Yamagata University School of Medicine, and written informed consent was obtained from all participants.

Follow-up of serological tests for liver function and fibrosis

The patients were followed up, and laboratory data were analyzed for 48 weeks in total, which included analyses once a month for 24 weeks before and after ABMi therapy. Patients who consumed more than 20 g alcohol/day during the analysis period were considered to have dropped out and excluded from further analysis. Primary outcomes were the safety and feasibility of ABMi therapy for ALC. The serum parameters representing liver function, including serum albumin, total protein, and prothrombin time, were evaluated before and after ABMi therapy. The Child-Pugh score calculated by summing the total points for the serum levels of albumin and total bilirubin, prothrombin time, ascites, and encephalopathy was used to evaluate the overall condition of patients with cirrhosis. To evaluate the changes in the degree of liver fibrosis in patients receiving ABMi, the serum levels of the type IV collagen 7S domain was monitored during the follow-up period. The liver function parameters of the control patients who succeeded in maintaining abstinence were followed up for the same period as that of patients who received ABMi.

Liver function calculated by single photon emission CT analysis

Analysis of the liver using single photon emission CT (SPECT) with a radiolabeled, specific hepatic binding protein, technetium 99m galactosyl-human serum albumin (Tc-GSA), was carried out according to the procedure we have previously reported [18]. SPECT analysis is useful for assessment of hepatic functional reserve [19,20]. Briefly, Tc-GSA (185 MBq) was injected intravenously, and SPECT data were obtained from 12 min 30 s to 17 min 30 s after the injection using a triple-headed camera (MULTISPECT 3; Siemens Medical Systems, Erlangen, Germany). The liver uptake ratio, that is, the actual percentage of the administered Tc-GSA dose incorporated into the liver, was quantified by calculating the percentage of the hepatic SPECT value relative to the preinjection syringe value. The liver volume was obtained from the SPECT data and calculated by the outline extraction method to determine the functional liver volume in cm^3. The liver uptake ratio was then divided by the functional liver volume to obtain the liver uptake ratio per unit volume (liver uptake density; %/cm^3). We assessed the obtained liver uptake density values of patients receiving ABMi before the treatment and 2 weeks after.

BM imaging by ^{111}In scintigraphy

BM scintigraphy using ^{111}In was performed in 4 of the 5 patients before and 1 week after ABMi therapy. BM scintigraphy is useful for evaluating the distribution of activated BM, mainly hematopoietic stem cells. The scintigraphy was conducted 48 h after an intravenous injection of ^{111}In (74 MBq). The total ^{111}In count was divided by the total number of pixels on the computer screen to obtain the ^{111}In

count per pixel, and this was used as an index of BM activation in patients before and 1 week after ABMi.

Statistical analysis

Statistical analysis was performed using *t*-test for paired or unpaired samples. Time courses of measurements of liver function parameters were analyzed by repeated-measures ANOVA. A 2-tailed *P* value of <0.05 was considered statistically significant. The data were expressed as mean ± standard error. Analyses were performed using SPSS version 15.0 for Windows (SRSS, Chicago, IL).

Results

Patients characteristics

Five patients received ABMi therapy and were followed up. The baseline demographic features and clinical characteristics of these 5 patients are shown in Table 1. All the patients were men with a mean age of 64 (range: 59–75) years. One patient had ascites, and the other 4 had a history of ascites. All patients had previously undergone endoscopic sclerosing therapy for esophageal varices. CT demonstrated macroscopic cirrhosis with a high degree of liver deformity, and all patients had undergone liver biopsy before the study, which confirmed cirrhosis histologically. The baseline data for the patients who received ABMi in comparison with those for the controls with alcoholic cirrhosis who were matched for age, sex, medication, and liver function parameters are shown in Table 2. There were no significant differences in these baseline data between the 2 groups.

Cell products for ABMi and their characteristics

The characteristics of the cell products for ABMi are shown in Table 3. From 400 mL of autologous BM harvested from the ilium of each patient, the mean number of infused MNCs was $8.0 \pm 7.3 \times 10^9$. The viability of the MNCs was >90% in all cases. The percentages of CD34+, CD44+, CD45+, and CD117+ cells were 6.0% ± 1.8%, 90.1% ± 5.6%, 81.2% ± 6.4%, and 12.0% ± 3.5%, respectively.

Changes in biochemical parameters before and after ABMi

The 5 patients receiving ABMi therapy were followed up for 48 weeks in total: for 24 weeks before and for 24 weeks after ABMi. The 5 controls were also followed up for a total of 48 weeks. Medication was not changed during the study period in any of the patients. The changes of liver function parameters, including serum albumin, total protein, and prothrombin time, are shown in Fig. 1. These parameters all showed an improvement in the patients who received ABMi; the mean level of serum albumin before and 24 weeks after ABMi improved from 3.3 ± 0.2 to 3.8 ± 0.2 g/dL, that of total protein improved from 6.9 ± 0.2 to 7.7 ± 0.1 g/dL, and the prothrombin time improved from 76.6% ± 6.1% to 87.6 % ± 6.0%. The levels of serum albumin, total protein, and prothrombin time during the follow-up period after ABMi were significantly higher than those during the period before ABMi (serum albumin; $P=0.02$, total protein; $P=0.03$, prothrombin time; $P<0.01$). However, no significant changes were observed in the levels of serum albumin and total protein, or prothrombin time, in the controls during the 48 weeks of observation. The Child-Pugh score decreased from 6.8 ± 1.3 before ABMi to 5.8 ± 0.8 at 24 weeks after ABMi. All of the 3 patients who were classified as Child class B with 7 points or higher before ABMi showed a decrease in their scores after ABMi therapy, and the remaining 2 patients classified as Child class A with 6 points or lower showed no change in their scores (Fig. 2).

Changes in liver fibrosis markers

The serum level of the type IV collagen 7S domain was evaluated in patients before and 24 weeks after ABMi. Improvement was observed in 4 of the 5 cases except for case no.5 at 24 weeks after ABMi therapy. The serum levels of the type IV collagen 7S domain decreased from 10.0 ± 3.9 ng/mL before to 8.1 ± 2.3 at 24 weeks after ABMi (Fig. 3), although the change was not significant ($P=0.33$), given the small number of cases examined.

Estimation of liver function using Tc-GSA SPECT

The functional index was improved at 2 weeks in 4 of the 5 patients who received ABMi therapy, and was unchanged in one (case no.1). The mean functional index calculated by Tc-GSA SPECT tended to increase from $2.4 \pm 0.5 \times 10^{-2}$ before ABMi to $2.7 \pm 0.6 \times 10^{-2}$ at 2 weeks after ($P=0.09$) (Fig. 4).

TABLE 1. PATIENT CHARACTERISTICS

							Serum markers					
	Age	*Sex*	*Etiology*	*Ascites*	*Coma*	*Varices*	*T.protein (g/dL)*	*Albumin (g/dL)*	*T.bilirubin (mg/dL)*	*PT (%)*	*ICG R15 (%)(K-ICG)*	*C-P score*
Patient 1	59	M	Alcohol	None (1)[a]	None (1)	positive[b]	6.5	2.7 (3)	1.0 (1)	67 (2)	40 (0.060)	8
Patient 2	61	M	Alcohol	None (1)[a]	None (1)	positive[b]	6.4	2.9 (2)	1.3 (1)	67 (2)	33 (0.077)	7
Patient 3	60	M	Alcohol	None (1)[a]	None (1)	positive[b]	6.7	3.8 (1)	0.8 (1)	92 (1)	27 (0.107)	5
Patient 4	75	M	Alcohol	None (1)[a]	None (1)	positive[b]	7.3	3.3 (2)	2.0 (2)	66 (2)	67 (0.043)	8
Patient 5	69	M	Alcohol	Minimal (2)	None (1)	positive[b]	7.7	3.7 (1)	1.5 (1)	91 (1)	46 (0.073)	6

Number in parentheses indicates points in total Child-Pugh (C-P) score.
[a]History of ascites.
[b]History of endoscopic sclerosing therapy.
T.protein, total protein; T.bilirubin, total bilirubin; PT, prothrombin time activity; ICG-R15, indocyanin green test, retention 15 min.

TABLE 2. BASELINE DATA OF AUTOLOGOUS BONE MARROW INFUSION GROUP AND CONTROL GROUP

Variable	ABMi group (n=5)	Control group (n=5)	P
Sex (male)	5	5	
Age (years)	64.6±2.9	61.2±4.5	N.S.
Total protein (g/dL)	6.92±0.25	7.22±0.38	N.S.
Serum albumin (g/dL)	3.28±0.22	3.28±0.06	N.S.
Total bilirubin (mg/dL)	1.36±0.20	1.38±0.25	N.S.
Prothrombin time (%)	76.6±6.1	84.8±7.2	N.S.
Medication			
Diuretics	3	3	
BCAA products	4	5	

N.S., not significant (*t*-test). The data are expressed by mean±standard error.

BCAA, branched chain amino acids; ABMi, autologous bone marrow infusion.

Activated BM distribution assessed by ^{111}In scintigraphy

The ^{111}In count per pixel was increased in 3 of the 4 patients tested at 1 week after ABMi therapy, but was not increased in case no.5. The average ^{111}In count per pixel in these 4 cases increased from 3.7±0.9 before ABMi to 4.4±1.3 at 1 week after (Fig. 5A), although the changes were not significant ($P=0.23$), given the small number of cases. The BM image in case no. 2, with the highest increase in the ^{111}In count after ABMi therapy, is shown in Fig. 5B. Activation of BM cells in case no.2 was demonstrated by an increase in the ^{111}In count per pixel from 4.5 before to 6.3 at 1 week after ABMi.

Complications

None of the 5 patients who received ABMi therapy exhibited any serious complications during or after the procedure.

Discussion

This study showed that ABMi for patients with ALC could be performed safely under general anesthesia and that it improved their liver function parameters including the serum levels of albumin and total protein and the prothrombin time. The Child-Pugh score also improved in all 3 patients who had a score higher than 7, which was classified as class B. Further, ABMi resulted in induction of hepatic functional reserve, as suggested by Tc-GSA SPECT imaging as well as reduction of the serum levels of the fibrosis marker in 4 of the 5 cases examined.

It is generally accepted that the results of laboratory tests can be modified by drug administration or infusion of albumin products or plasma. Although both patients treated with ABMi and controls had received several types of medication, the administered drugs were not changed during the study period, whereas the patients abstained from alcohol and no blood products were supplied. Abstinence is an important factor to consider when selecting patients for ABMi, because ALC is an irreversible liver condition resulting from chronic inflammation attributable to the toxic effect of ethanol on the liver. For enrollment in the present study, patients who showed marked deformity of the liver on CT, and histologically proved cirrhosis, were required to have abstained from alcohol for at least 24 weeks. No changes in liver function parameters were found as a result of an abstinence in either the controls or the patients treated with ABMi in the period before ABMi. However, the results of the present study suggest that liver function parameters can be improved by ABMi in patients with ALC. A recent study has shown that patients who undergo orthotropic liver transplantation for alcoholic liver disease have a rate of recidivism as high as 28% at 9 years [21]. Therefore, both careful observation and adequate intervention in relation to abstinence may be required for patients after ABMi.

Although BM stem cell treatment for liver cirrhosis is an attractive strategy in the field of liver regenerative cell therapy, many concerns need to be addressed [22,23]. It is still unclear how infused BM cells work for the improvement of liver function. We have demonstrated experimentally that BM cells transplanted into the spleen of rats with liver damage induced by carbon tetrachloride express liver-specific proteins such as alpha-fetoprotein in their cytoplasm in the recipient liver [10]. A clinical trial of ABMi for patients with cirrhosis has also demonstrated that the number of alpha-fetoprotein-positive cells was increased significantly in the liver, relative to the situation before ABMi. In addition, ABMi appeared to induce hepatocyte proliferation in the liver, as expression of proliferating cell nuclear antigen, a marker of hepatocyte proliferation, was significantly increased after ABMi in comparison with the pretreatment situation [15]. Another study has shown that intraportal administration of autologous CD133+ BM cells and subsequent portal venous embolization of right liver segments resulted in a 2.5-fold increase in the mean proliferation rate of the left lateral segment, in comparison with controls not

TABLE 3. CHARACTERISTICS OF PROCESSED MONONUCLEAR CELLS

	Harvest vol. (mL)	No. of infused MNCs ($X\ 10^9$)	CD34+ (%)	CD44+ (%)	CD45+ (%)	CD117+ (%)
Patient 1	400	3.0	4.3	87.7	85.2	10.9
Patient 2	400	2.5	8.8	84.4	78.8	15.9
Patient 3	400	16.0	5.2	93.7	82.4	8.2
Patient 4	400	2.3	5.2	97.9	88.0	15.5
Patient 5	400	16.0	6.7	86.6	71.4	9.6
Mean±SE		8.0±7.3	6.0±1.8	90.1±5.6	81.2±6.4	12.0±3.5

MNC, mononuclear cell.

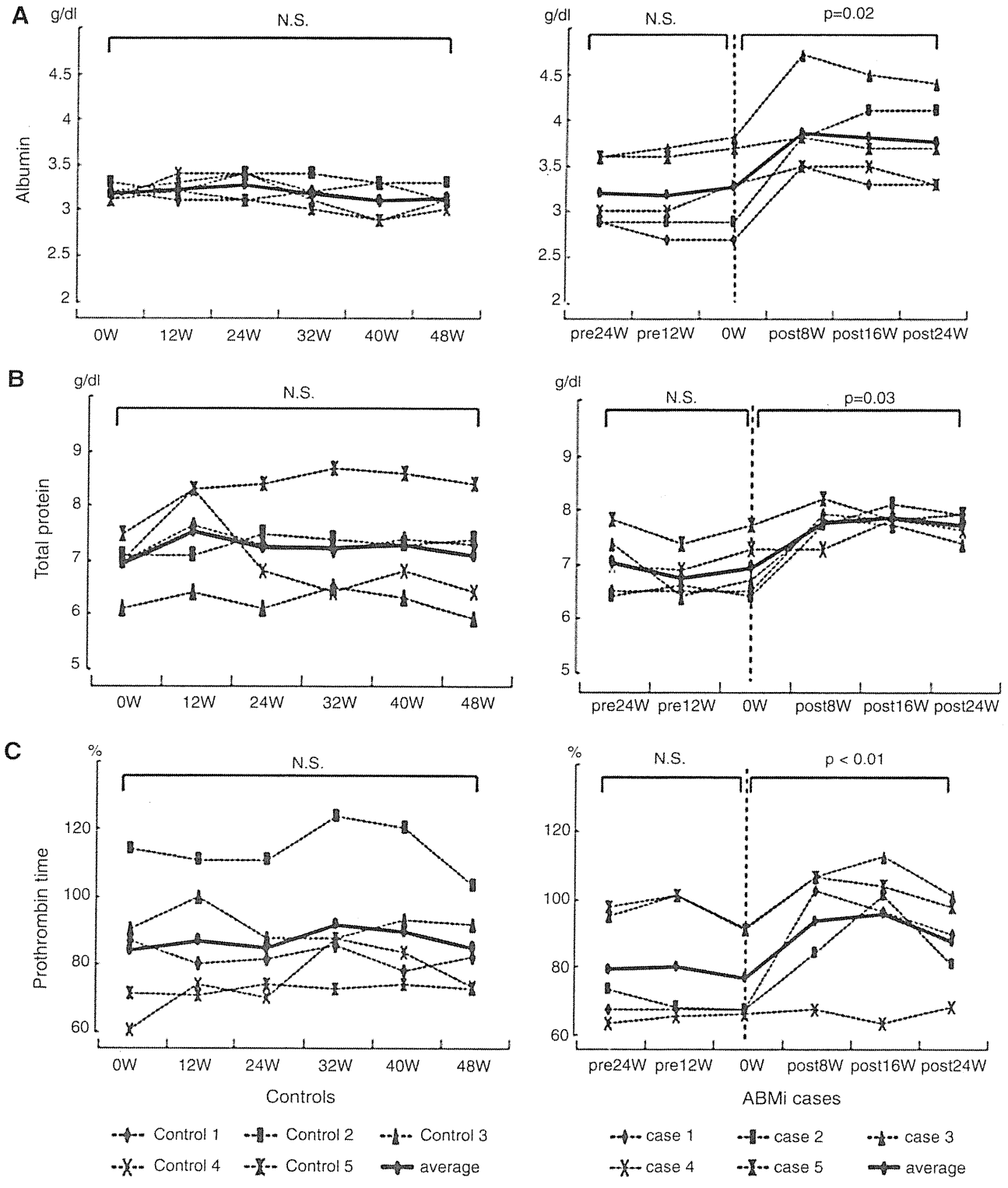

FIG. 1. Changes in biochemical parameters before and after ABMi. The levels of serum albumin (A) and total protein (B), and prothrombin time (C), during the follow-up of patients after ABMi were significantly higher than those during the period before ABMi. No significant changes were observed in the controls. ABMi, autologous bone marrow infusion.

receiving BM transfusion [24]. These data suggest that transplanted BM cells have a potential role in liver regeneration and proliferate in the recipient liver and that this process is likely to occur early after ABMi, as Tc-GSA SPECT analysis in the present study demonstrated an increase in the liver function index of most patients 2 weeks after ABMi. However, since it is still unclear whether fully functional hepatocytes are induced by ABMi, the characteristics of BM

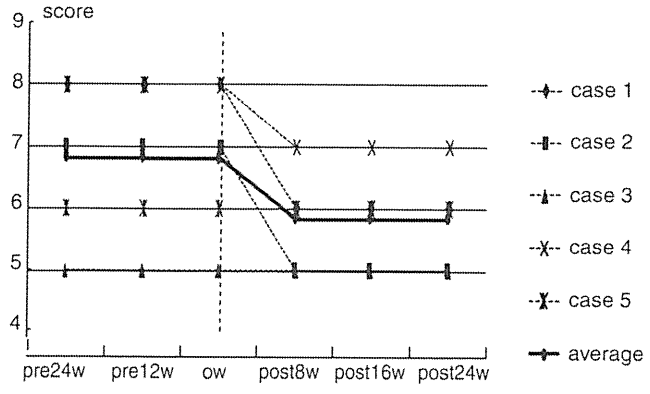

FIG. 2. Changes in Child-Pugh score after ABMi in comparison with those before. The Child-Pugh score decreased from 6.8±1.3 before ABMi to 5.8±0.8 at 24 weeks after ABMi. All of the 3 patients classified as class B, scoring 7 points or higher before ABMi, showed a decrease in their scores after the therapy.

stem cells that show hepatocyte differentiation should be elucidated further. In addition, to elucidate the cell-cell communication in the extracellular microenvironment that would be important for tissue repair, many markers originating from the different cell types among MNCs should be investigated in the future.

The tracking of BM cells infused into the human body as a means of monitoring cell engraftment after ABMi has not been previously reported. In the present study, BM scintigraphy using ^{111}In before and after ABMi showed that the distribution of activated BM was enhanced systemically after ABMi, including the liver, in 3 of the 4 patients examined. Although the process of migration of infused BM cells to the liver remains unknown, clarification of the factors responsible could yield important data for improving the efficiency of transplantation. In fact, ABMi case no. 2, in which the greatest increase in the ^{111}In count was observed 1 week after ABMi, showed a marked decrease in the concentration of the

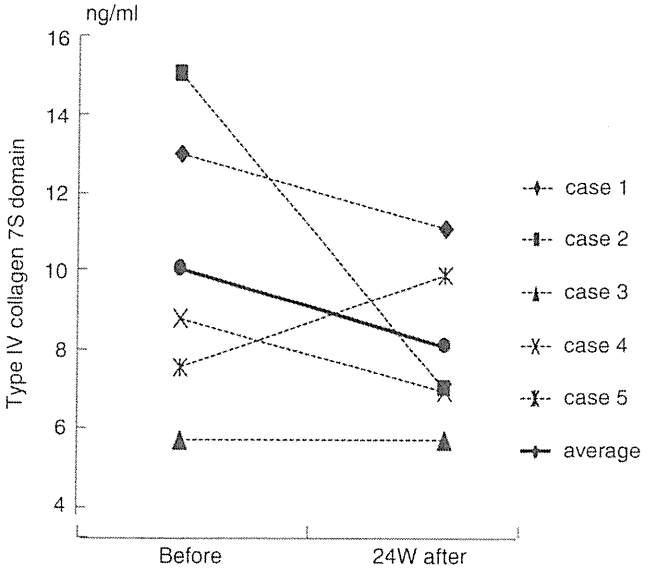

FIG. 3. Changes in the levels of a liver fibrosis marker after ABMi in comparison with those before. The level of the type IV collagen 7S domain improved in 4 of the 5 cases, with the exception of case no.5, at 24 weeks after ABMi therapy, and their serum levels decreased from 10.0±3.9 ng/mL before to 8.1±2.3 ng/mL at 24 weeks after the therapy.

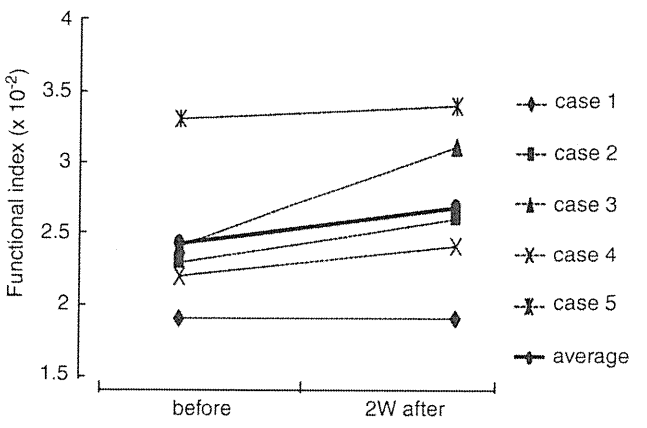

FIG. 4. Estimation of liver function using technetium 99m galactosyl-human serum albumin single photon emission computed tomography. The functional index improved in 4 of the 5 cases, and did not change in one (case 1) after ABMi. The mean functional index tended to increase from $2.4\pm0.5\times10^{-2}$ before ABMi to $2.7\pm0.6\times10^{-2}$ at 2 weeks after ($P=0.09$).

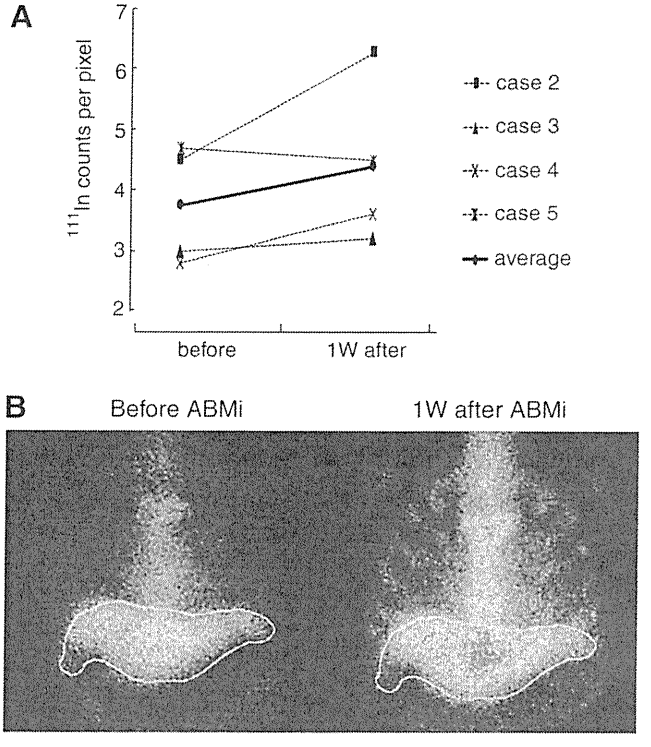

FIG. 5. Activated BM distribution demonstrated by indium-111-chloride (^{111}In) scintigraphy. **(A)** The ^{111}In count per pixel increased in 3 of the 4 patients tested after ABMi therapy, with the exception of case no.5. The average ^{111}In count per pixel in the 4 patients increased from 3.7±0.9 before to 4.4±1.3 after ABMi. **(B)** BM image of case no. 2, showing the greatest increase of the ^{111}In count 1 week after ABMi therapy (4.5 before to 6.3 after).

type IV collagen 7S domain, as shown in Fig. 3, as well as a marked improvement of liver function parameters, as shown in Fig. 1. In contrast, ABMi case no.5 was only one showing no change in the ^{111}In count at 1 week after ABMi, and the only case in which the level of the type IV collagen 7S domain did not decrease after ABMi. Effective migration of infused BM cells to the liver may ameliorate liver fibrosis, because such cells have been shown experimentally to produce and secrete anti-fibrosis factors such as matrix metalloproteinase-9 [7]. At this time, the factors that determine the difference between effectiveness and noneffectiveness are unclear. Collateral circulation resulting from the portal vein disorganization that characterizes liver cirrhosis may affect the flow and effective migration of infused BM cells to the liver, and, thus, migration of infused cells to the liver may partly depend on the portal venous pressure. Further, the expression levels of cellular adhesion molecules associated with the attachment of infused cells to liver tissue may vary a great deal among patients. It is important to determine the adhesion molecules that are induced in the liver tissue of patients receiving ABMi. Further studies are needed to clarify the mechanisms involved in the migration of infused BM cells to the liver.

The present study did not demonstrate the long-term effectiveness of this therapy in terms of survival rate or improvement in the quality of life. Such effects will need to be evaluated by a randomized controlled study in the future. In addition, improvements in the methods of delivering infused BM cells to the human body should also be investigated further. We are currently conducting experiments aimed at improving the effectiveness of this therapy by investigating the long-term culture conditions for BM cells, the optimum cell population to be employed, the effectiveness of repeated transplantation of BMCs, and the optimum route of cell delivery. We have already confirmed both the safety and short-term efficacy of ABMi therapy for various liver diseases [15,16], and these basic data are expected to be of value for improving ABMi therapy in the near future.

In summary, ABMi therapy for patients with alcoholic cirrhosis has been shown to improve liver function parameters, in contrast to observation accompanied by abstinence from alcohol. The markers of liver fibrosis, hepatic functional reserve, and BM cell activation were improved in most of the patients who received ABMi therapy. However, the degree of effectiveness of ABMi is likely to differ among patients, and the present results should still be considered in terms of a pilot study. Further investigation of factors associated with the effectiveness of this therapy is warranted, and future studies will need to assess the safety of this therapy and its effect on liver function in a large number of patients, together with its long-term effectiveness, in terms of survival rate and quality of life.

Acknowledgments

This study was supported in part by a grant from the Ministry of Health, Labor, and Welfare of Japan, and also in part by a Grant-in-Aid from the Global COE program of the Japan Society for the Promotion of Science. The authors thank Dr. K. Okita for his support toward this study.

Author Disclosure Statement

The authors declare that they have no conflict of interest.

References

1. Krause K, C Schneider, KH Kuck and K Jaquet. (2010). Stem cell therapy in cardiovascular disorders. Cardiovasc Ther 28:e101–e110.
2. Bui QT, ZM Gertz and RL Wilensky. (2010). Intracoronary delivery of bone-marrow-derived stem cells. Stem Cell Res Ther 1:29.
3. Petersen BE, WC Bowen, KD Patrene, WM Mars, AK Sullivan, N Murase, SS Boggs, JS Greenberger and JP Goff. (1999). Bone marrow as a potential source of hepatic oval cells. Science 284:1168–1170.
4. Alison MR, R Poulsom, R Jeffery, AP Dhillon, A Quaglia, J Jacob, M Novelli, G Prentice, J Williamson and NA Wright. (2000). Hepatocytes from non-hepatic adult stem cells. Nature 406:257.
5. Theise ND, S Badve, R Saxena, O Henegariu, S Sell, JM Crawford and DS Krause. (2000). Derivation of hepatocytes from bone marrow cells in mice after radiation-induced myeloablation. Hepatology 31:235–240.
6. Theise ND, M Nimmakayalu, R Gardner, PB Illei, G Morgan, L Teperman, O Henegariu and DS Krause. (2000). Liver from bone marrow in humans. Hepatology 32:11–16.
7. Sakaida I, S Terai, N Yamamoto, K Aoyama, T Ishikawa, H Nishina and K Okita. (2004). Transplantation of bone marrow cells reduces CCl4-induced liver fibrosis in mice. Hepatology 40:1304–1311.
8. Terai S, I Sakaida, N Yamamoto, K Omori, T Watanabe, S Ohata, T Katada, K Miyamoto, K Shinoda, H Nishina and K Okita. (2003). An in vivo model for monitoring transdifferentiation of bone marrow cells into functional hepatocytes. J Biochem 134:551–558.
9. Okumoto K, T Saito, E Hattori, JI Ito, A Suzuki, K Misawa, R Ishii, T Karasawa, H Haga, M Sanjo, T Takeda, K Sugahara, K Saito, H Togashi and S Kawata. (2005). Differentiation of rat bone marrow cells cultured on artificial basement membrane containing extracellular matrix into a liver cell lineage. J Hepatol 43:110–116.
10. Okumoto K, T Saito, E Hattori, JI Ito, A Suzuki, K Misawa, M Sanjyo, T Takeda, K Sugahara, K Saito, H Togashi and S Kawata. (2005). Expression of Notch signaling markers in bone marrow cells that differentiate into a liver cell lineage in a rat transplanted model. Hepatol Res 31:7–12.
11. Okumoto K, T Saito, H Haga, E Hattori, R Ishii, T Karasawa, A Suzuki, K Misawa, M Sanjo, JI Ito, K Sugahara, K Saito, H Togashi and S Kawata. (2006). Characteristics of rat bone marrow cells differentiated into a liver cell lineage and dynamics of the transplanted cells in the injured liver. J Gastroenterol 41:62–69.
12. Haga H, T Saito, K Okumoto, S Ugajin, C Sato, R Ishii, Y Nishise, J Ito, H Watanabe, K Saito, H Togashi and S Kawata. (2011). Enhanced expression of fibroblast growth factor 2 in bone marrow cells and its potential role in the differentiation of hepatic epithelial stem-like cells into hepatocyte lineage. Cell Tissue Res 343:371–378.
13. Gordon MY, N Levicar, M Pai, P Bachellier, I Dimarakis, F Al-Allaf, H M'Hamdi, T Thalji, JP Welsh, SB Marley, J Davies, F Dazzi, F Marelli-Berg, P Tait, R Playford, L Jiao, S Jensen, JP Nicholls, A Ayav, M Nohandani, F Farzaneh, J Gaken, R Dodge, M Alison, JF Apperley, R Lechler and NA Habib. (2006). Characterization and clinical application of human CD34+ stem/progenitor cell populations mobilized into the blood by granulocyte colony-stimulating factor. Stem Cells 24:1822–1830.

14. Levicar N, M Pai, NA Habib, P Tait, LR Jiao, SB Marley, J Davis, F Dazzi, C Smadja, SL Jensen, JP Nicholls, JF Apperley and MY Gordon. (2008). Long-term clinical results of autologous infusion of mobilized adult bone marrow derived CD34+ cells in patients with chronic liver disease. Cell Prolif 41 (Suppl 1):115–125.
15. Terai S, T Ishikawa, K Omori, K Aoyama, Y Marumoto, Y Urata, Y Yokoyama, K Uchida, T Yamasaki, Y Fujii, K Okita and I Sakaida. (2006). Improved liver function in patients with liver cirrhosis after autologous bone marrow cell infusion therapy. Stem Cells 24:2292–2298.
16. Kim JK, YN Park, JS Kim, MS Park, YH Paik, JY Seok, YE Chung, HO Kim, KS Kim, SH Ahn, DY Kim, MJ Kim, KS Lee, CY Chon, SJ Kim, S Terai, I Sakaida and KH Han. (2010). Autologous bone marrow infusion activates the progenitor cell compartment in patients with advanced liver cirrhosis. Cell Transplant 19:1237–1246.
17. Pai M, D Zacharoulis, MN Milicevic, S Helmy, LR Jiao, N Levicar, P Tait, M Scott, SB Marley, K Jestice, M Glibetic, D Bansi, SA Khan, D Kyriakou, C Rountas, A Thillainayagam, JP Nicholls, S Jensen, JF Apperley, MY Gordon and NA Habib. (2008). Autologous infusion of expanded mobilized adult bone marrow-derived CD34+ cells into patients with alcoholic liver cirrhosis. Am J Gastroenterol 103:1952–1958.
18. Sugahara K, H Togashi, K Takahashi, Y Onodera, M Sanjo, K Misawa, A Suzuki, T Adachi, J Ito, K Okumoto, E Hattori, T Takeda, H Watanabe, K Saito, T Saito, Y Sugai and S Kawata. (2003). Separate analysis of asialoglycoprotein receptors in the right and left hepatic lobes using Tc-GSA SPECT. Hepatology 38:1401–1409.
19. Kudo M, A Todo, K Ikekubo, K Yamamoto, DR Vera and RC Stadalnik. (1993). Quantitative assessment of hepatocellular function through in vivo radioreceptor imaging with technetium 99m galactosyl human serum albumin. Hepatology 17:814–819.
20. Kwon AH, SK Ha-Kawa, S Uetsuji, Y Kamiyama and Y Tanaka. (1995). Use of technetium 99m diethylenetriaminepentaacetic acid-galactosyl-human serum albumin liver scintigraphy in the evaluation of preoperative and postoperative hepatic functional reserve for hepatectomy. Surgery 117:429–434.
21. Biselli M, A Gramenzi, M Del Gaudio, M Ravaioli, G Vitale, S Gitto, GL Grazi, AD Pinna, P Andreone and M Bernardi; Bologna Liver Transplantation Group. (2010). Long term follow-up and outcome of liver transplantation for alcoholic liver disease: a single center case-control study. Clin Gastroenterol 44:52–57.
22. Kallis YN, MR Alison and SJ Forbes. (2007). Bone marrow stem cells and liver disease. Gut 56:716–724.
23. Lorenzini S and P Andreone. (2007). Stem cell therapy for human liver cirrhosis: a cautious analysis of the results. Stem Cells 25:2383–2384.
24. am Esch JS 2nd, WT Knoefel, M Klein, A Ghodsizad, G Fuerst, LW Poll, C Piechaczek, ER Burchardt, N Feifel, V Stoldt, M Stockschläder, N Stoecklein, RY Tustas, CF Eisenberger, M Peiper, D Häussinger and SB Hosch. (2005). Portal application of autologous CD133+ bone marrow cells to the liver: a novel concept to support hepatic regeneration. Stem Cells 23:463–470.

Address correspondence to:
Dr. Takafumi Saito
Department of Gastroenterology
Yamagata University School of Medicine
2-2-2 Iida-nishi
Yamagata 990-9585
Japan

E-mail: tasaitoh@med.id.yamagata-u.ac.jp

Received for publication February 16, 2011
Accepted after revision March 20, 2011
Prepublished on Liebert Instant Online March 20, 2011

Ann Nucl Med (2011) 25:520–523
DOI 10.1007/s12149-011-0484-0

CASE REPORT

^{99m}Tc-GSA SPECT analysis was clinically useful to evaluate the effect of interferon in a patient with interferon non-responsive chronic hepatitis C

Rika Ishii · Hitoshi Togashi · Akiko Iwaba · Chikako Sato · Hiroaki Haga · Mai Sanjo · Kazuo Okumoto · Yuko Nishise · Jun-itsu Ito · Hisayoshi Watanabe · Koji Saito · Akio Okada · Kazuei Takahashi · Takafumi Saito · Sumio Kawata

Received: 15 December 2010 / Accepted: 23 February 2011 / Published online: 2 April 2011

Abstract We describe a 62-year-old woman with advanced chronic hepatitis C who showed no response to low-dose long-term interferon-beta monotherapy (3 MU, three times a week). The interferon monotherapy was continued for 2 years and 9 months. Despite this lack of response to interferon, the patient's clinical course was good and liver function assessed by ^{99m}Tc-galactosyl human serum albumin single photon emission computed tomography (^{99m}Tc-GSA SPECT) analysis improved significantly. Improvement of the data obtained by ^{99m}Tc-GSA SPECT analysis justified continuation of the treatment. ^{99m}Tc-GSA SPECT analysis was clinically useful to evaluate the effect of interferon in a patient with interferon non-responsive chronic hepatitis C, despite a lack of reduction of the ALT level and HCV-RNA titer.

Keywords Chronic hepatitis C · Interferon non-responder · ^{99m}Tc-GSA SPECT

R. Ishii · H. Togashi · C. Sato · H. Haga · M. Sanjo · K. Okumoto · Y. Nishise · J. Ito · H. Watanabe · K. Saito · T. Saito · S. Kawata
Department of Gastroenterology, Yamagata University Faculty of Medicine, 2-2-2 Iida-nishi, Yamagata 990-9585, Japan

H. Togashi (✉)
Yamagata University Health Administration Center, 1-4-12 Kojirakawa-machi, Yamagata 990-8560, Japan
e-mail: htogashi@med.id.yamagata-u.ac.jp

A. Iwaba
Department of Pathological Diagnostics, Yamagata University Faculty of Medicine, 2-2-2 Iida-nishi, Yamagata 990-9585, Japan

A. Okada · K. Takahashi
Department of Radiology, Yamagata University Faculty of Medicine, 2-2-2 Iida-nishi, Yamagata 990-9585, Japan

Introduction

Hepatitis C virus (HCV) usually causes chronic infection, which can result in chronic hepatitis, liver cirrhosis, and hepatocellular carcinoma over the course of several decades [1]. However, effective treatment is available. Interferon (IFN) is able to eradicate HCV and can induce marked biochemical and histological improvement [2]. The current standard therapy for chronic HCV infection is a combination of pegylated IFN and ribavirin [3]. In patients with high viral loads of genotype 1, the rate of sustained virological response is about 50% for this combination treatment. However, patients who do not respond, or in whom the treatment fails because of severe complications, are referred for new treatment options. Although low-dose long-term interferon (IFN maintenance) therapy has been attempted as a new treatment option, its efficacy in terms of liver function and histology has varied markedly among previous reports [4–7]. The real-time evaluation of IFN therapy in patients with chronic hepatitis C who are truly IFN-non-responsive during the therapy will help in justifying the validity of continuation of IFN therapy.

The asialoglycoprotein receptor (ASGPR) is abundantly expressed on the sinusoidal surface of the hepatocytes adjacent to the extracellular space of Disse in the liver. It is tempting to speculate that the ASGPR may be a relevant factor in the inflammation and fibrosis associated with chronic viral hepatitis. We have developed ^{99m}Tc-GSA SPECT analysis that can evaluate regional hepatic function and the progression of chronic viral hepatitis using dynamic changes in ASGPRs [8]. Here, we report a patient with chronic hepatitis C who received interferon-beta (IFN-β) maintenance therapy, and whose liver function and histology improved significantly, even though the ALT level was not controllable and the viral load did not

decrease during the therapy. Improvement of the data obtained by ^{99m}Tc-GSA SPECT analysis justified continuation of the treatment.

Case report

A 62-year-old woman was admitted to our hospital for further examination of liver dysfunction on April 10, 2002. Liver biochemical tests showed elevated levels of aspartate aminotransferase (AST 69 IU/l) and alanine aminotransferase (ALT 68 IU/l). The patient was seronegative for all hepatitis B virus markers, but seropositive for anti-HCV by a third-generation enzyme immunoassay. The HCV-RNA titer was high (>850 KIU/ml) and the genotype was 1b (Table 1). Liver biopsy was performed on April 12, 2002, and this demonstrated severe fibrosis and moderate inflammation activity in portal areas (Fig. 1a, b). On April 16, 2002, ^{99m}Tc-GSA SPECT was performed, and this indicated that liver uptake ratio (LUR) and liver uptake density (LUD) of the whole liver were 74 and 0.048%/ml, respectively. The patient had no history of excessive alcohol intake, and was diagnosed as having advanced chronic hepatitis C. In 1995, she received natural IFN-α monotherapy in other hospital, but the monotherapy was withdrawn after 3 months because of non-response and adverse effects. When considering the therapeutic history, we planned to treat the patient with recombinant interferon alpha-2b (IFN-α2b: Intron A, Schering-Plough, Kenilworth, NJ), 6 MU daily for 2 weeks, and then three times a week for an additional 22 weeks in combination with peroral ribavirin at 600 mg/day [Revetol, Schering-Plough (RBV)]. From April 22, 2002, 6 MU of IFN-α2b combined with 600 mg/day RBV was started. The combination therapy was continued, by adjusting the dosage of IFN-α2b and RBV in accordance with any adverse effects, such as leukocytopenia and thrombocytopenia. However, as the patient was non-responsive to the recombinant IFN-α2b and RBV combination therapy, it was withdrawn on November 25, 2002 (Fig. 2).

Table 1 Laboratory data at first admission

WBC	3,670/μl	TP	7.4 g/dl	FBS	83 mg/dl
RBC	4.07×10^6	ALB	4.4 g/dl	T-Cho	174 mg/dl
Hb	13.4 g/dl	ZTT	8.7 IU/l	TG	91 mg/dl
Ht	39.9%	T-BIL	0.6 mg/dl	AFP	7.4 ng/ml
Plt	11.0×10^3/μl	D-BIL	0.2 mg/dl		
PT	132.4%	AST	69 IU/l	HBsAg	(−)
Na	146 mEq/l	ALT	68 IU/l	HCV-Ab	(+)
K	4.4 mEq/l	LDH	412 IU/l	HCV-RNA	>850 KIU/ml
Cl	105 mEq/l	ALP	87 IU/l	HCV genotype	1b
BUN	14 mg/dl	γ-GTP	28 IU/l		
CREA	0.7 mg/dl	ChE	411 IU/l		
UA	4.6 mg/dl				

AFP alpha-fetoprotein, *ALB* albumin, *ALP* alkaline phosphatase, *ALT* alanine aminotransferase, *AST* aspartate aminotransferase, *BUN* blood urea nitrogen, *ChE* cholinesterase, *Cl* chloride, *CREA* creatine, *D-Bil* direct bilirubin, *γ-GTP* gamma glutamyl transpeptidase, *Hb* hemoglobin, *HBsAg* hepatitis B virus surface antigen, *HCV-Ab* hepatitis C virus antibody, *HCV-RNA* hepatitis C virus RNA, *Ht* hematocrit, *K* potassium, *LDH* lactate dehydrogenase, *Na* sodium, *Plt* platelets, *PT* prothrombin time, *RBC* red blood cells, *T-Bil* total bilirubin, *T-Chol* total cholesterol, *TG* triglyceride, *TP* total protein, *UA* uric acid, *WBC* white blood cells, *ZTT* zinc sulfate turbidity test

We previously reported that ^{99m}Tc-GSA SPECT analysis was clinically useful in evaluating regional hepatic function and the progression of chronic viral hepatitis using dynamic changes in the asialoglycoprotein receptors [8]. On April 13, 2004, ^{99m}Tc-GSA SPECT analysis was performed, and the indices obtained, LUR and LUD, which reflect the amount and density of asialoglycoprotein receptors in the liver, respectively, were found to be decreased considerably during the 2 years' follow-up period (Fig. 1c). The LUR correlated particularly well with conventional liver function tests, and LUD was a good indicator of periportal and/or bridging necrosis and fibrosis [8]. The patient was diagnosed as having advanced chronic hepatitis.

On July 1, 2004, 3 MU of IFN-β (IFN-β: Toray Co., Tokyo), three times a week, was administered intravenously to improve the function of the liver, as the ALT level remained at more than 50 IU/l and the patient strongly desired IFN maintenance therapy. IFN-β was used because of fewer side effects when compared with IFN-α. The written informed consent was obtained before the start of the IFN-β therapy. In contrast to our expectation, however, the ALT level did not decrease after induction of the IFN-β maintenance therapy, and remained at over 50 IU/l. Moreover, the HCV-RNA titer increased. The IFN-β maintenance therapy was continued because the patient had no serious complications, and compliance was satisfactory. On March 10, 2005, ^{99m}Tc-GSA SPECT analysis was performed again, and this indicated that LUR and LUD of the whole liver were 74 and 0.046%/ml, respectively, suggesting a significant improvement. On March 30, 2007, IFN-β maintenance therapy was completed after a total duration of 2 years and 9 months (Fig. 2).

Thereafter, ALT gradually decreased (Fig. 2). Repeat ^{99m}Tc-GSA SPECT analysis at 1 year after the completion of INF-β maintenance therapy indicated further improvement of LUR and LUD (Fig. 3a). The LUR and the LUD values for whole liver and right lobes recovered to the mean values for normal control group. Liver biopsy was also conducted 1 year after the completion of IFN-β maintenance therapy (October 1, 2008), and the histology showed significant improvement of hepatic fibrosis and diminished portal inflammation (Fig. 3b, c). Throughout

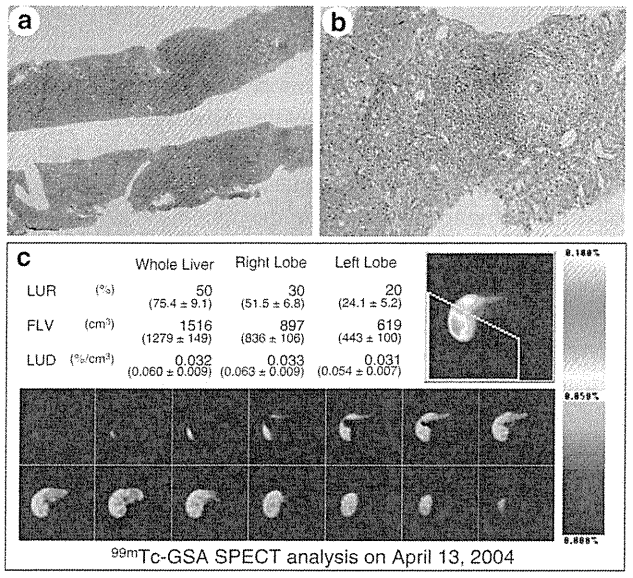

Fig. 1 Histopathology and ^{99m}Tc-GSA SPECT analysis. **a** and **b** Histopathology of the liver on April 12, 2002. Severe hepatic fibrosis and moderate inflammatory activity in the portal areas are evident. **a** Elastica–Masson staining, ×4 magnification with objective lens. **b** H&E staining, ×20 magnification with objective lens. **c** Images and data from ^{99m}Tc-GSA SPECT analysis conducted on April 13, 2004. A decrease in the liver uptake ratio of ^{99m}Tc-GSA and the expression of ASGPRs was demonstrated. Mean and standard values for normal control group are indicated in *parentheses*. The patient was diagnosed as having advanced chronic hepatitis

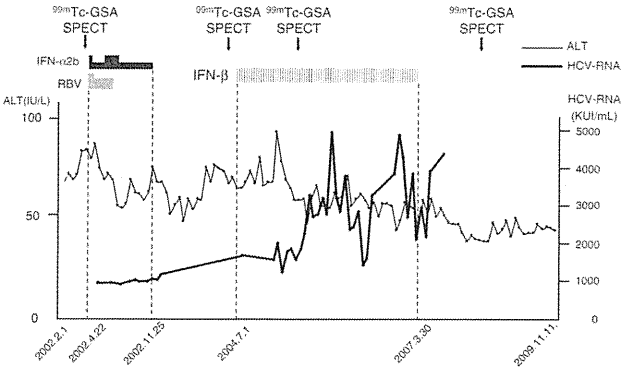

Fig. 2 Clinical course of the patient. On April 22, 2002, recombinant IFN-α2b and RBV combination therapy was started by adjusting the dosage of IFN-α2b and RBV in accordance with adverse effects. The therapy was continued until November 25, 2002. The patient was non-responsive to the combination therapy. Because the ALT level remained high (>60 IU/l), we introduced IFN-β maintenance therapy, but the ALT level and HCV-RNA titer did not decrease at all. However, ^{99m}Tc-GSA SPECT analysis performed on March 10, 2005, showed a significant improvement of hepatic functional reserve. IFN-β maintenance therapy was continued for a total of 2 years and 9 months. After completion of the therapy, the ALT level gradually decreased and the patient's condition has been good up to the time of writing

the clinical course, she was administered ursodeoxycholic acid (300 mg/day per orally), but was not administered angiotensin-converting enzyme inhibitors, AT1-receptor

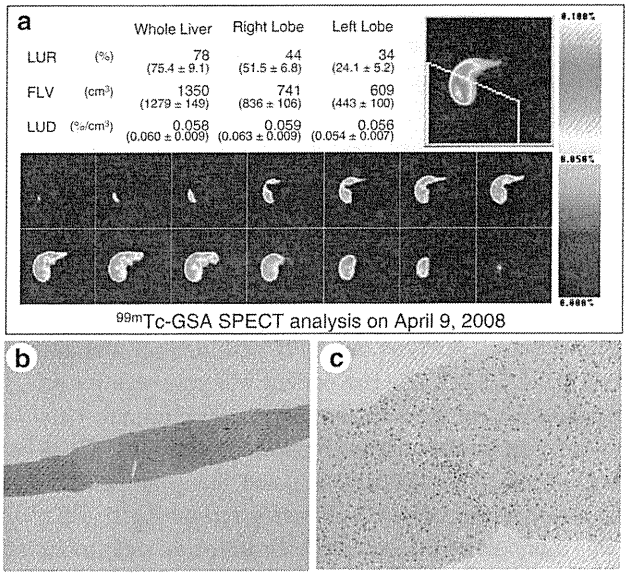

Fig. 3 ^{99m}Tc-GSA SPECT analysis and histopathology. **a** Images and data from ^{99m}Tc-GSA SPECT analysis conducted on April 9, 2008. After 1 year of completion of IFN-β monotherapy, ^{99m}Tc-GSA SPECT indicated an increase in LUR and LUD in comparison with the data obtained on March 10, 2005 and April 13, 2004 (Fig. 1c), indicating a significant improvement of liver function. **b**, **c** Histopathology of a liver biopsy obtained on October 1, 2008. One year and 7 months after the completion of IFN-β monotherapy, the histopathology showed a decrease of hepatic fibrosis and diminished hepatic inflammation, suggesting a significant improvement. **b** Elastica–Masson staining, ×4 magnification with objective lens. **c** H&E staining, ×20 magnification with objective lens

blockers, nor glycyrrhizin injection. The patient's clinical course has since remained favorable, and the ALT level has been controllable with no sign of hepatocellular carcinoma up to the time of writing.

Discussion

The present case of chronic hepatitis C showed resistance to previously performed IFN-α2b and ribavirin combination therapy. As a new option for this difficult-to-treat patient, we administered 3 MU of IFN-β three times per week intravenously. After IFN-β induction, there was no decline of transaminase levels, and the HCV-RNA titer increased somewhat. Because there were no adverse complications and the patient's compliance was satisfactory, we continued the maintenance therapy for a further 2 years and 9 months, anticipating that the IFN-β would have an anti-fibrotic effect [9], in parallel with the confirmation of liver function by ^{99m}Tc-GSA SPECT analysis. Even after withdrawal of the maintenance IFN-β therapy, the patient's condition has been good, and the results of ^{99m}Tc-GSA SPECT analysis and liver biopsy histology have improved considerably.